An unbiased tissue transcriptome analysis identifies potential markers for skin phenotypes and therapeutic responses in atopic dermatitis

Ayano Fukushima-Nomura, Eiryo Kawakami, Masayuki Amagai et al.

Supplementary Figure 1.

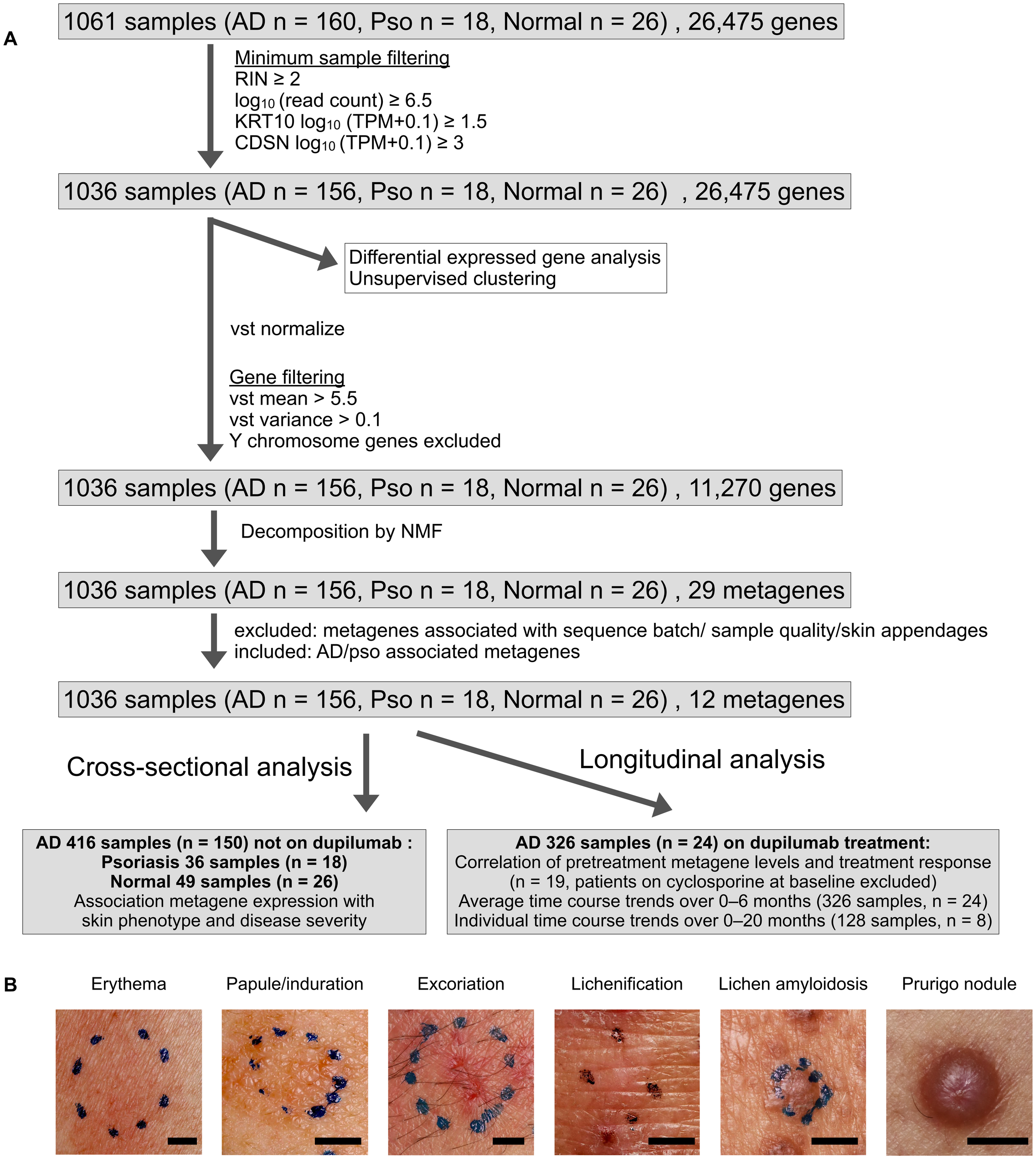

Supplementary Figure 1. Study flow diagram and symptoms of sampled skin.
A) Flowchart detailing the exclusion and inclusion criteria of samples, genes, and metagenes derived from NMF. AD: atopic dermatitis; Pso: psoriasis; n: number of individuals; NMF: non-matrix factorization method; vst: variance stabilizing transformation. B) Examples of skin pathology of samples from AD patients. The images were taken at approximately the same magnification. Samples from “excoriation” sites were taken from the epithelialized site adjacent to the erosions. The black bar represents 5 mm.

Supplementary Figure 2.

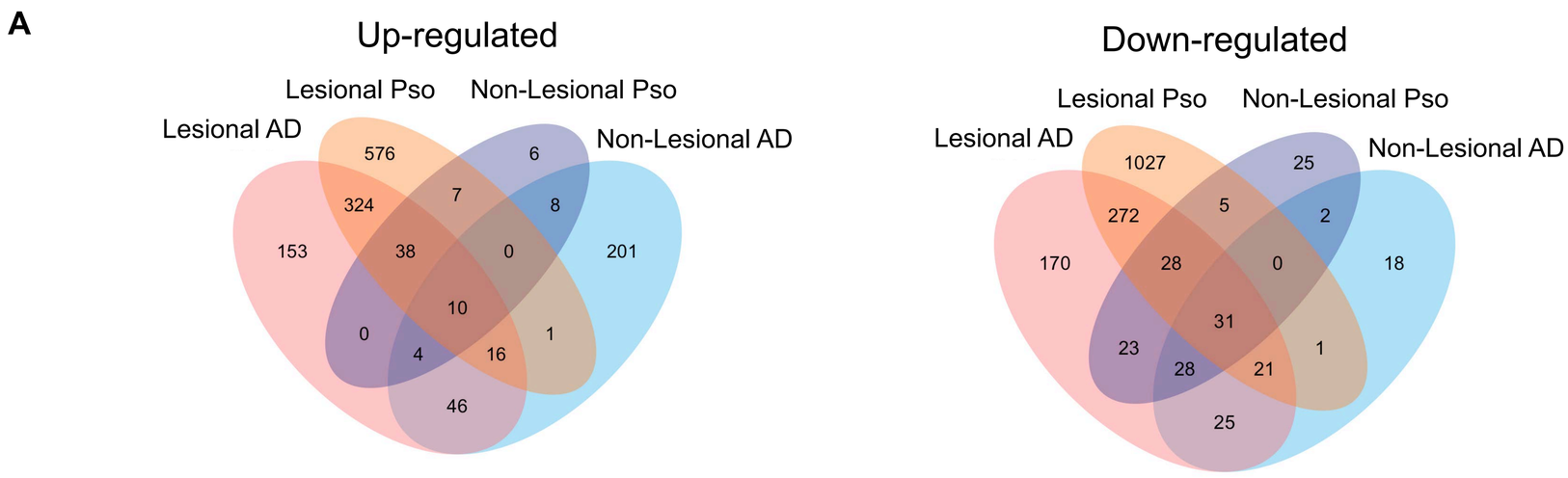

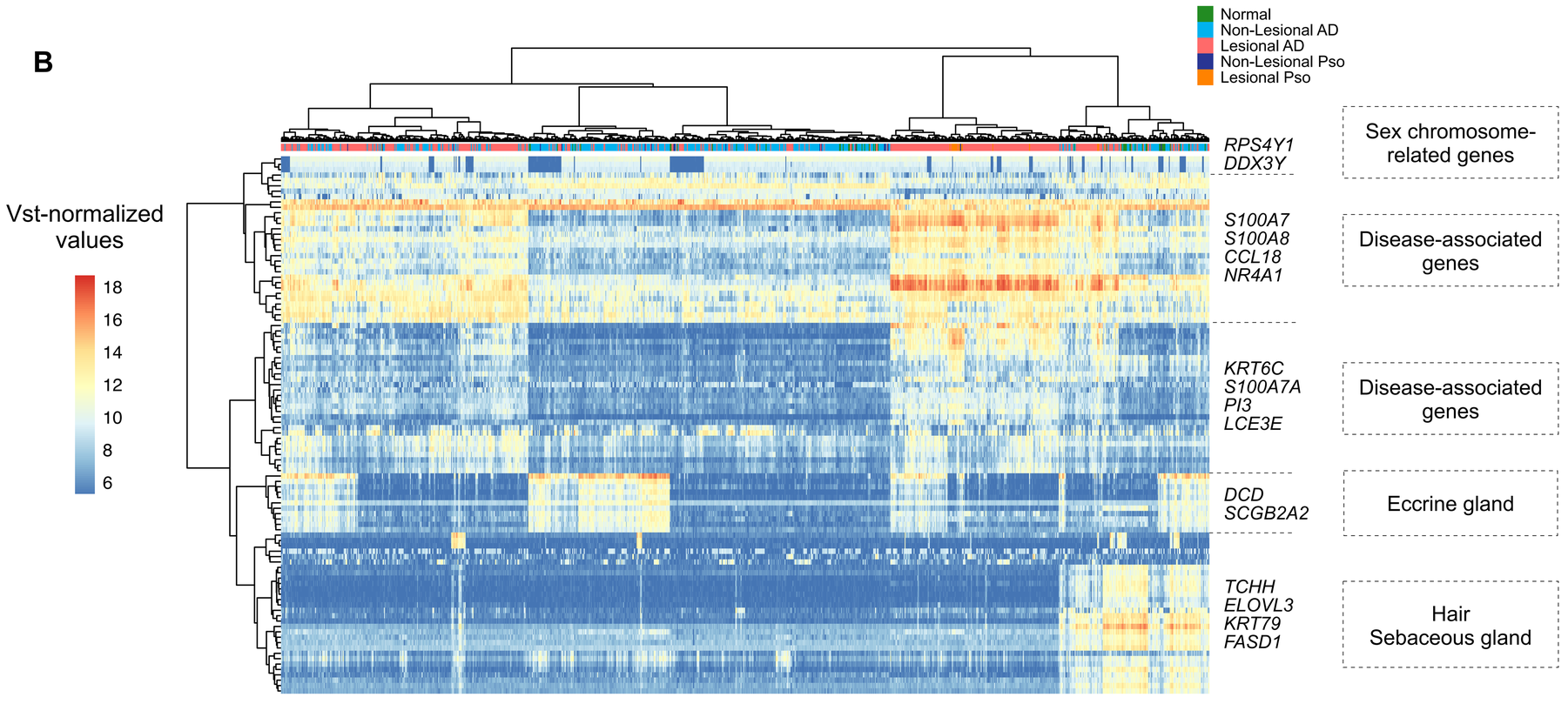

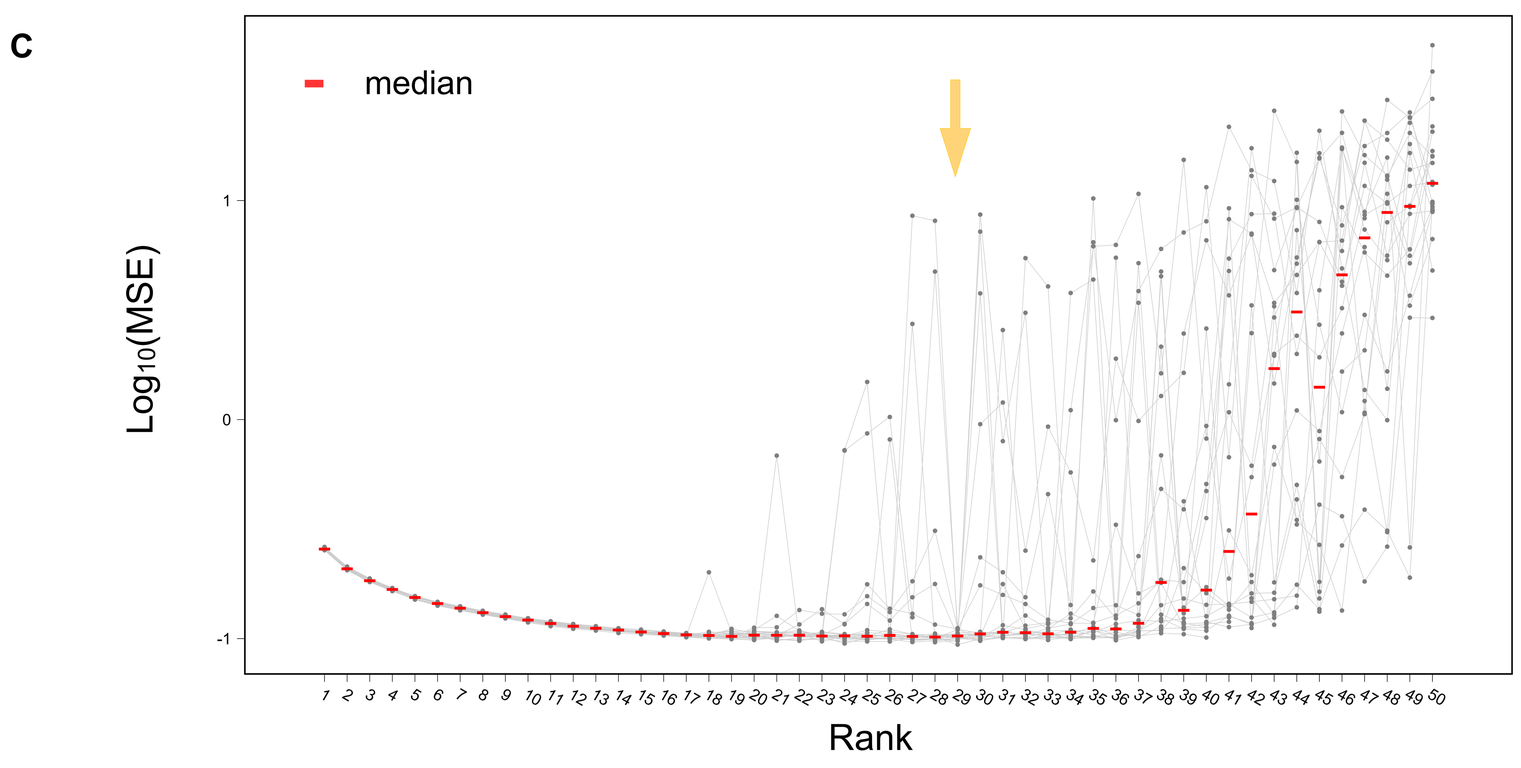

Supplementary Figure 2. Hierarchical clustering analysis and non-negative matrix factorization (NMF) analysis of skin samples.
A) Venn diagram of differentially expressed genes between samples in different groups relative to the normal samples. B) Skin appendage gene expression overrides the diversity of gene expression in skin affected by atopic dermatitis (AD) in the hierarchical clustering results. Variance-stabilizing transformation (vst)-normalized values of the top 100 variant genes were used for this analysis. Clustering was performed using the ward.D2 method and the Euclidean distance. Almost half of the most variant genes were derived from skin appendages. n = 1036 samlples. C) The median reconstruction error for ranks 1 to 50 of the NMF analysis. A model at k = 29 was selected for the analysis.

Supplementary Figure 3.

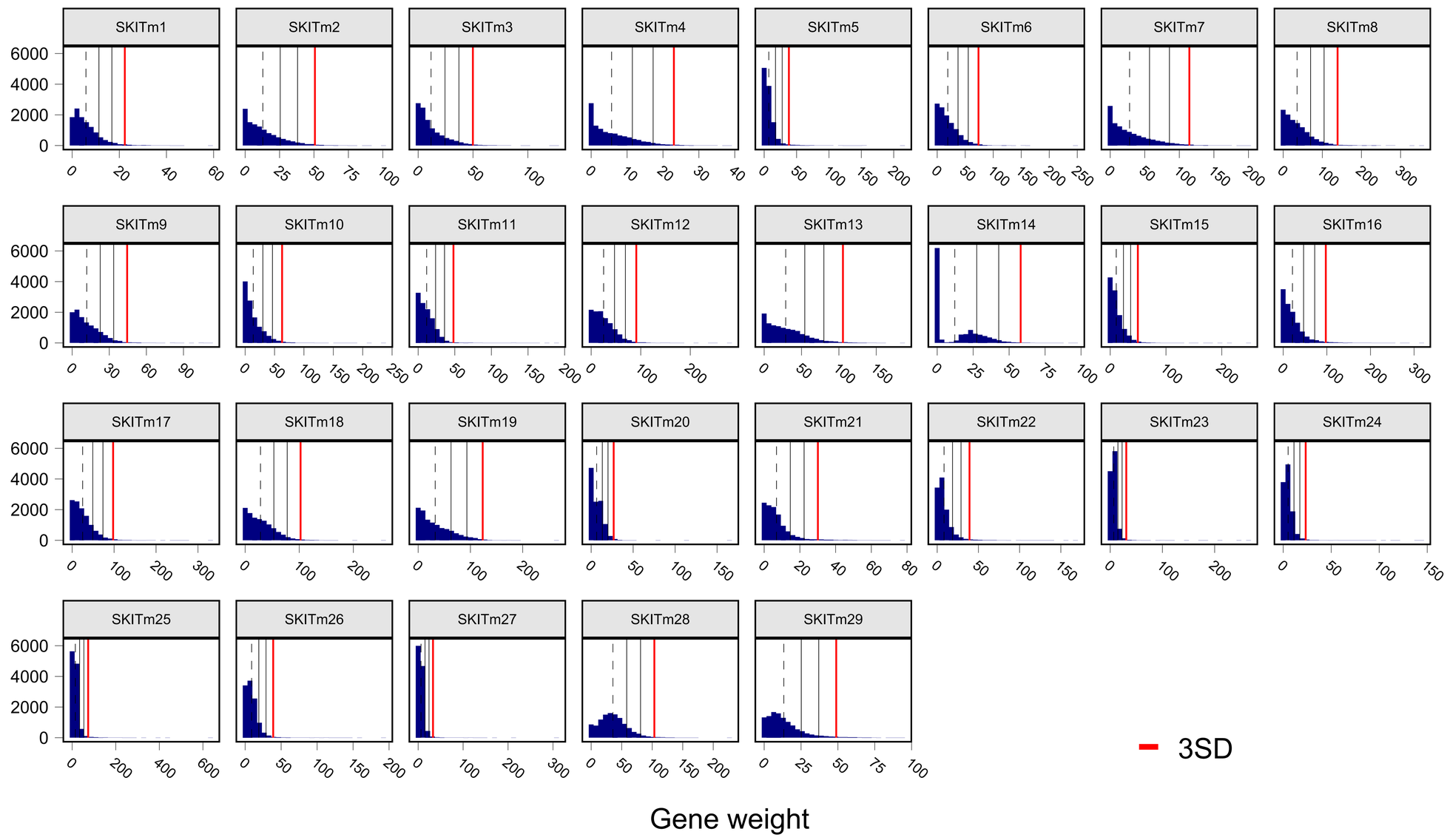

Supplementary Figure 3. Distribution of gene weights and expression of metagenes obtained using non-negative matrix factorization (NMF) analysis.
Distribution of gene weights for each metagene. The mean (dashed lines), 1 SD and 2 SD values (black lines), and 3 SD values (red lines) of gene weights for each metagene are depicted. Genes with weights greater than 3 SD values were selected as “highly-weighted genes”. n = 1036 samples.

Supplementary Figure 4.

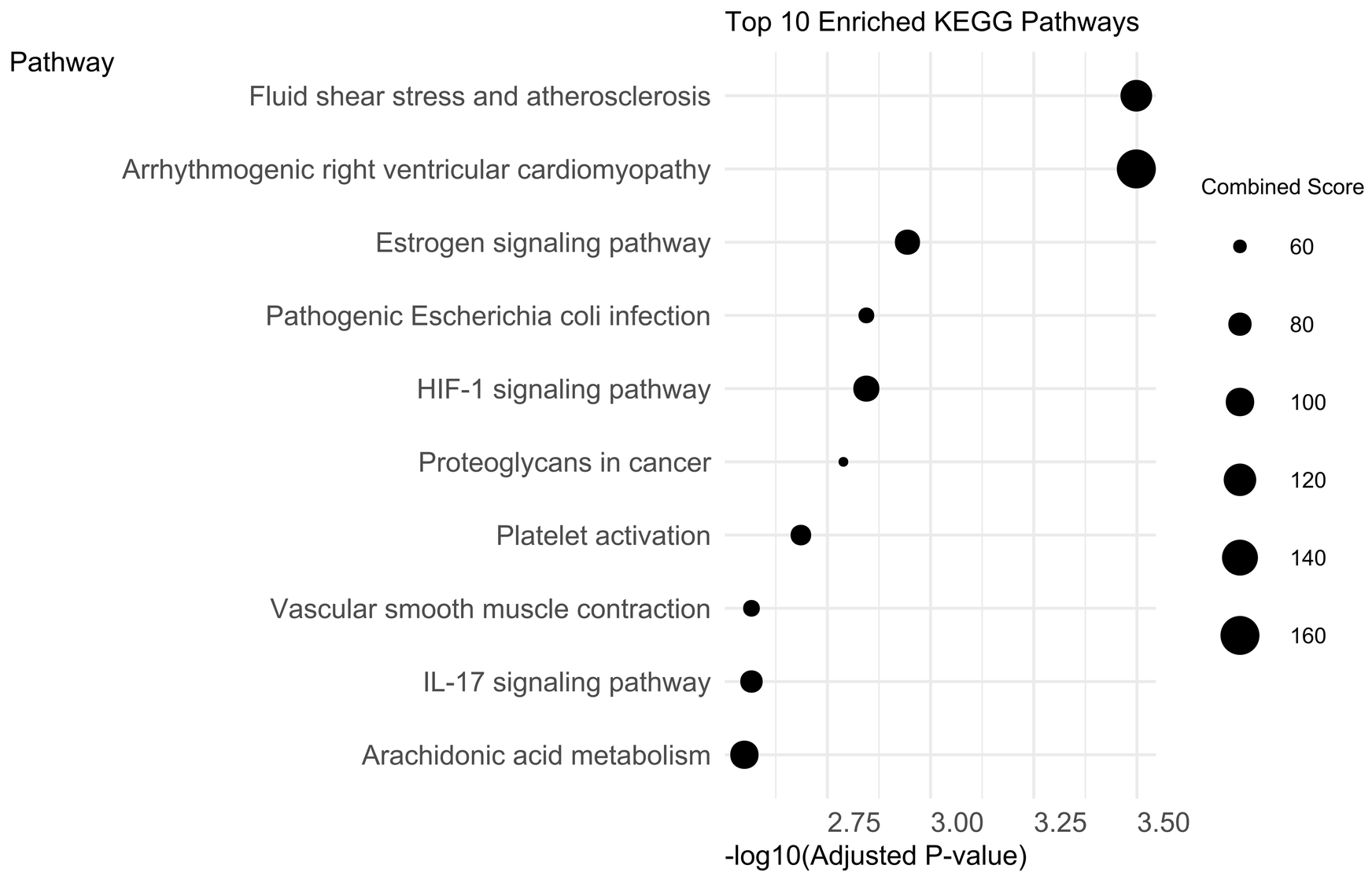

Supplementary Figure 4. Example of biological annotation of skin metagene.

Enrichment analysis of the highly-weighted genes in SKITm10 using the KEGG pathway database.

Supplementary Figure 5.

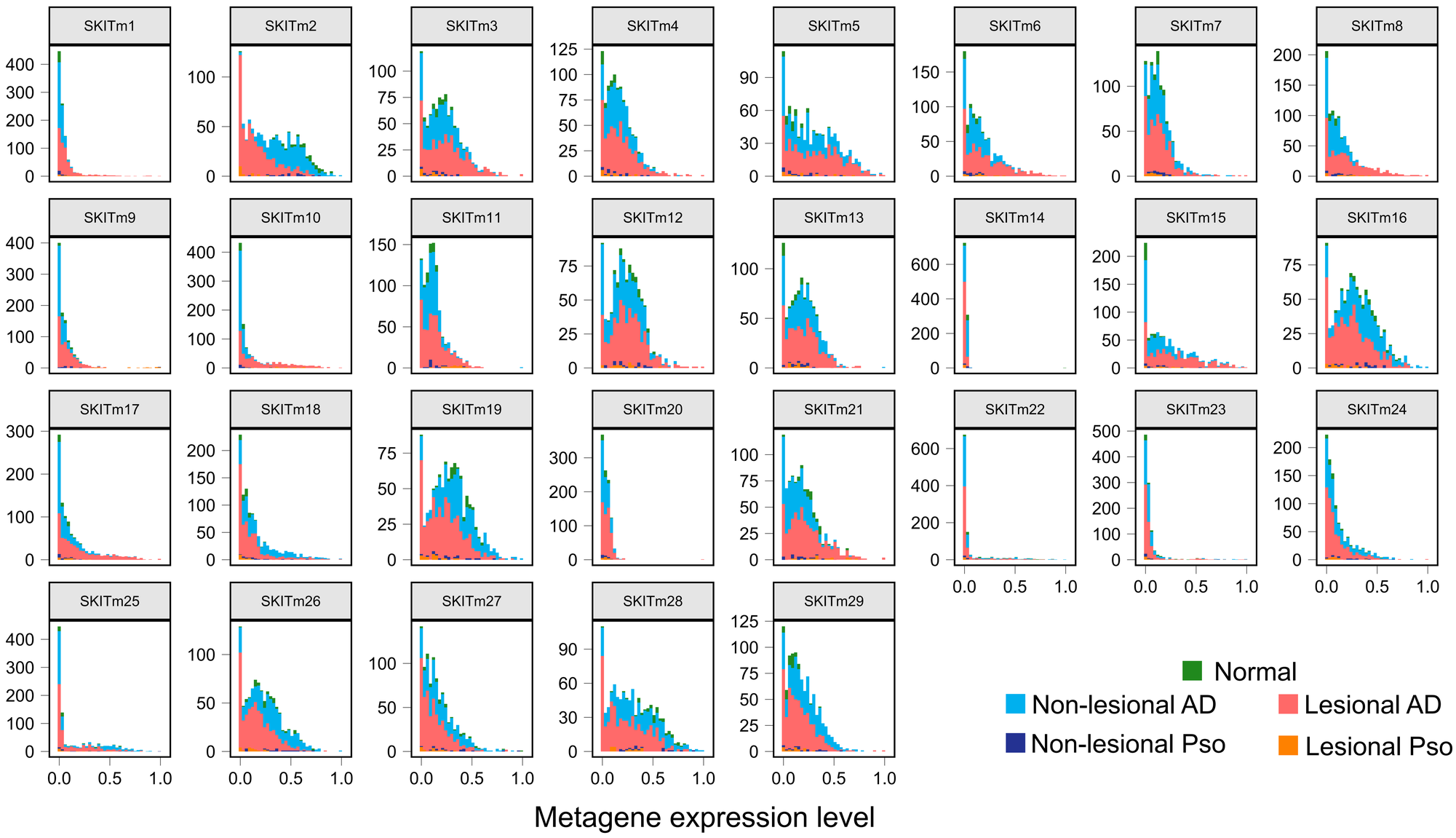

Supplementary Figure 5. Distribution of the metagene expression values in the skin samples.

Supplementary Figure 6.

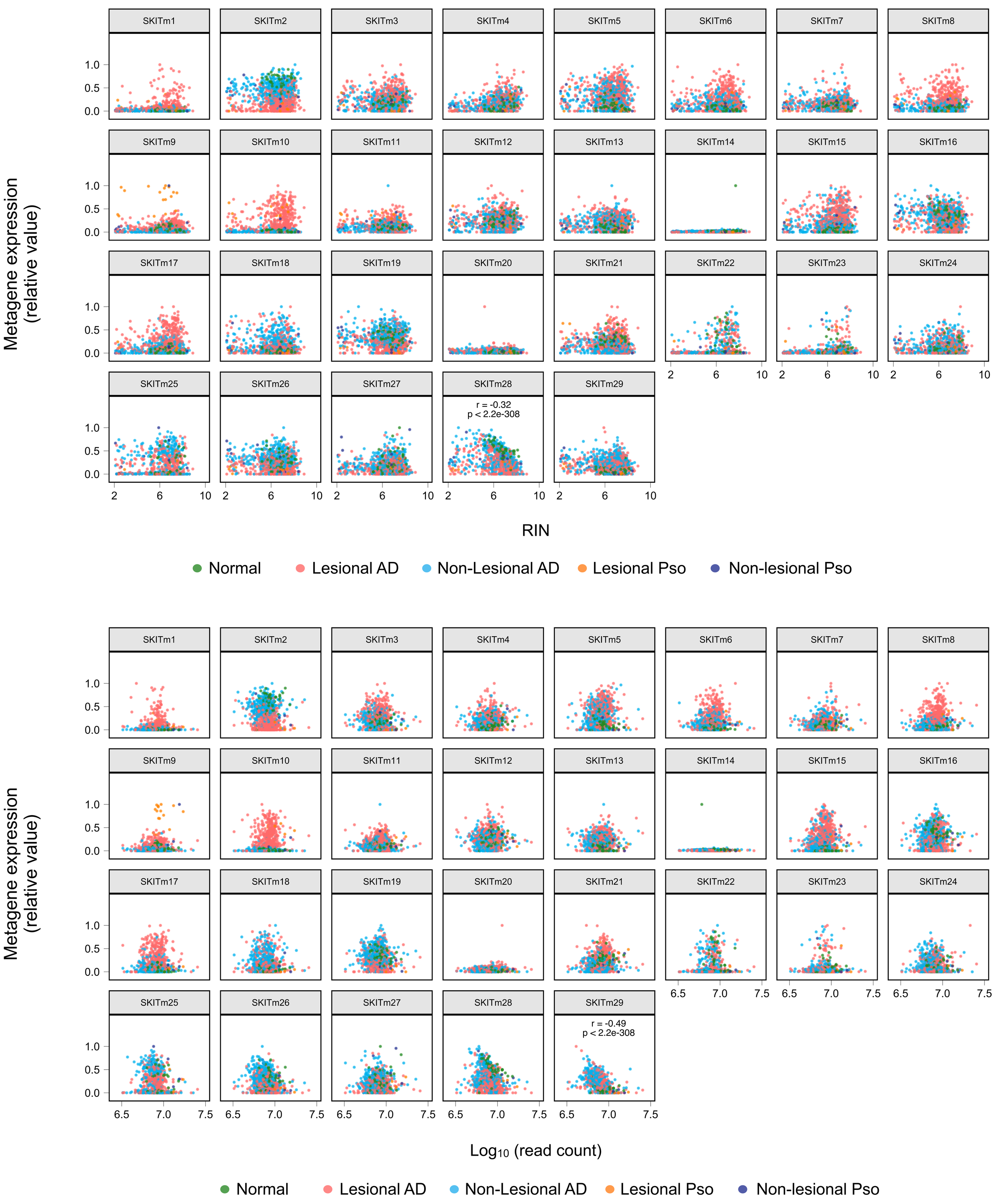

Supplementary Figure 6.

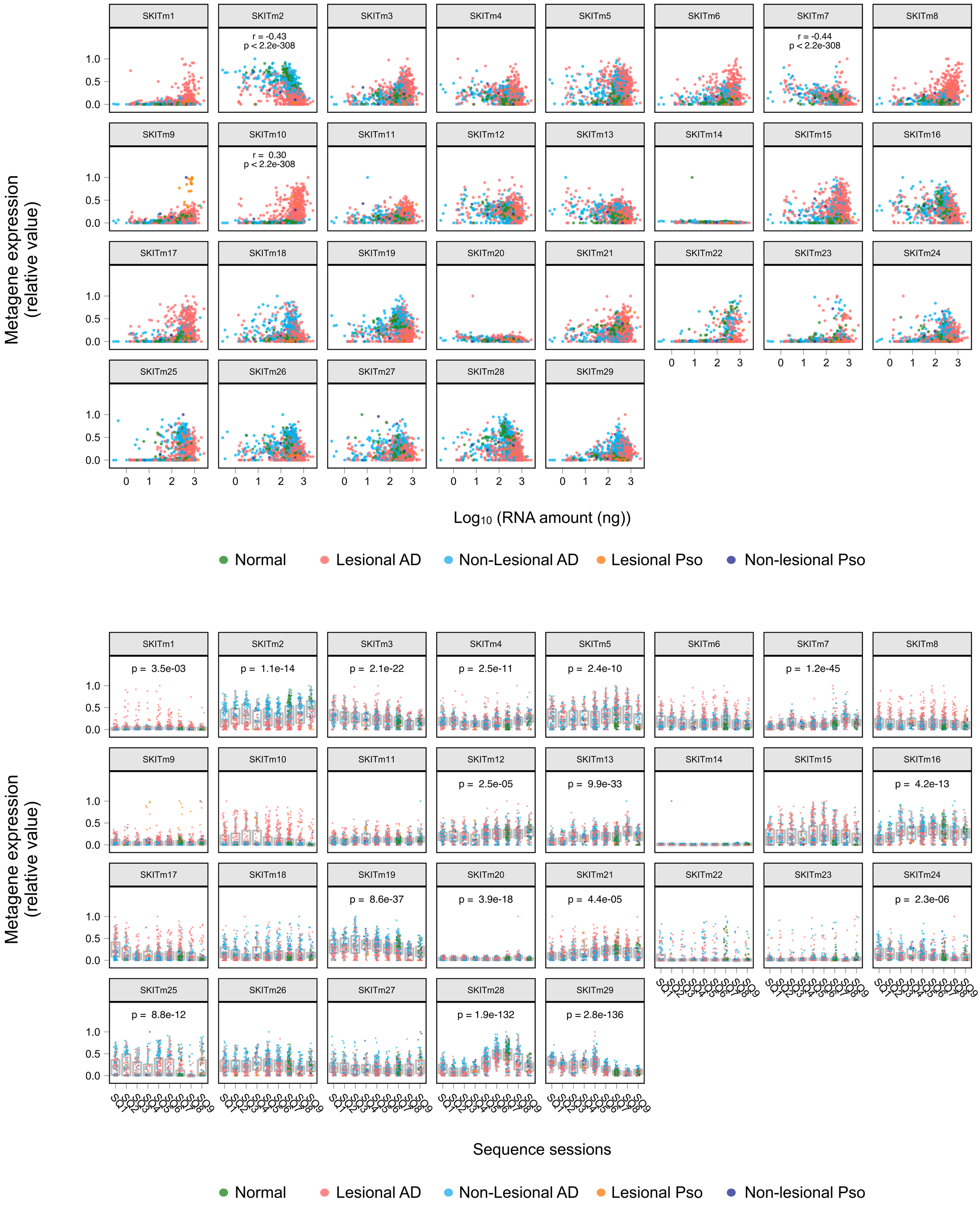

Supplementary Figure 6. Analysis of skin metagenes associated with sample quality and batch effect.
In all figures, each dot represents a single sample. For A), B) and C), r and p indicate the Pearson correlation coefficient and its corresponding significance, respectively. Only results with correlation coefficients greater than 0.3 or less than −0.3 are shown. P-values were adjusted for multiple comparisons using the Bonferroni correction. A) SKITm28 expression was negatively correlated with RIN (RNA integrity number). n = 1036 samples. B) SKITm29 expression was negatively correlated with sequencing read depth. n = 1036 samples. C) SKITm2, SKITm7, and SKITm10 expression levels were negatively correlated with the extracted RNA volume. n = 1029 samples. D) Metagene expression across sequence sessions. P-values indicate the significance of the effect of sequence sessions on metagene expression obtained by regression analysis . To evaluate the batch effect from RNA sequencing, samples processed in nine separate sequencing sessions (SQ1–SQ9) were analyzed. Two linear models were compared: one including the sequencing session as an explanatory variable and one excluding it. These models were fitted using the lm function and compared by ANOVA test. The p-value from this comparison is shown in the figure and indicates whether sequencing session had a significant effect on gene expression.
The p-values were corrected using the Bonferroni method for multiple comparisons. n = 1036 samples. Source data are provided as a Source Data file.

Supplementary Figure 7.

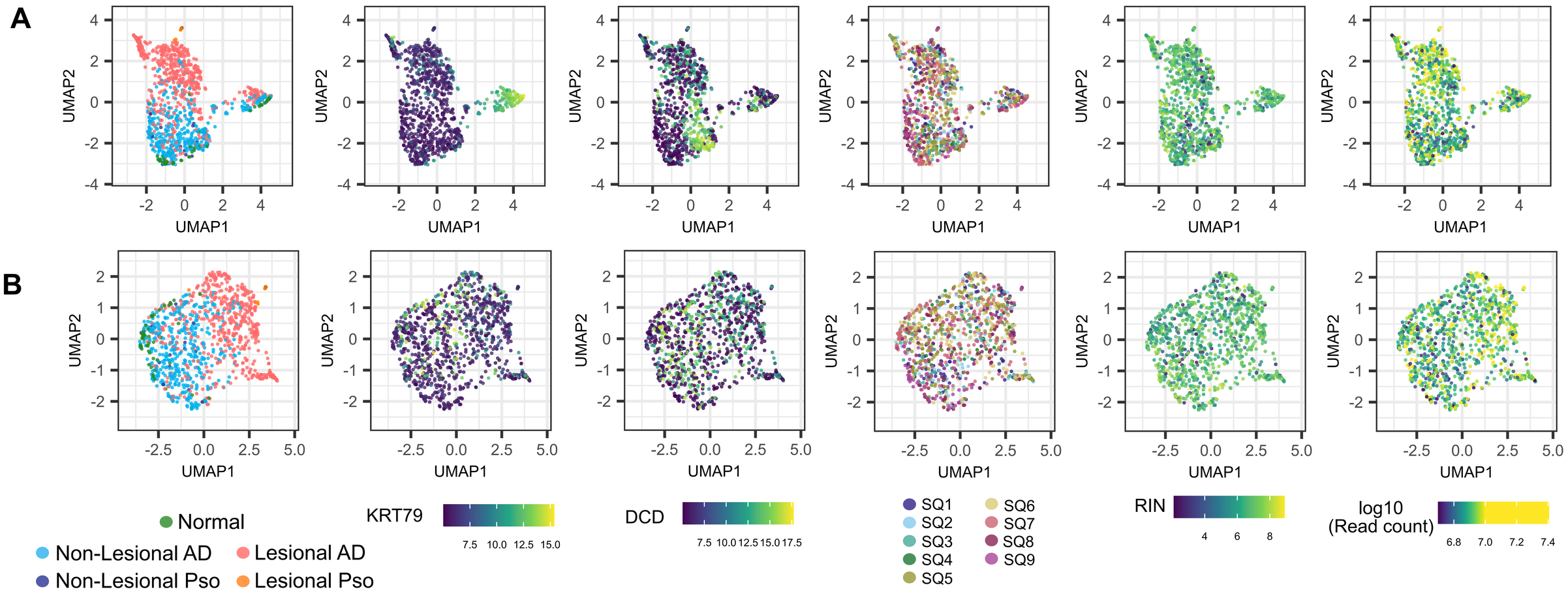

Supplementary Figure 7. Effect of exclusion of metagenes associated with sample bias. A) Uniform Manifold Approximation and Projection (UMAP) analysis was conducted based on the expression of all 29 metagenes. B) UMAP analysis conducted based on the expression of 18 metagenes. Eleven sample-bias-related metagenes were excluded: skin appendage and reticulocyte inclusion (SKITm22–27, SKITm19), sample outliers (SKITm14, SKITm20), sample quality and batch effects (SKITm28, SKITm29). In A), some clusters reflect the high expression of *KRT79* (a marker of sebaceous glands), *DCD* (a marker of sweat glands), and sequence sessions. These clusters become less conspicuous in B). n (samples) = 49 (normal), 529 (lesional AD), 422 (non-lesional AD), 18 (lesional psoriasis), and 18 (non-lesional psoriasis). RIN: RNA integrity number; SQ: sequence sessions.

Supplementary Figure 8.

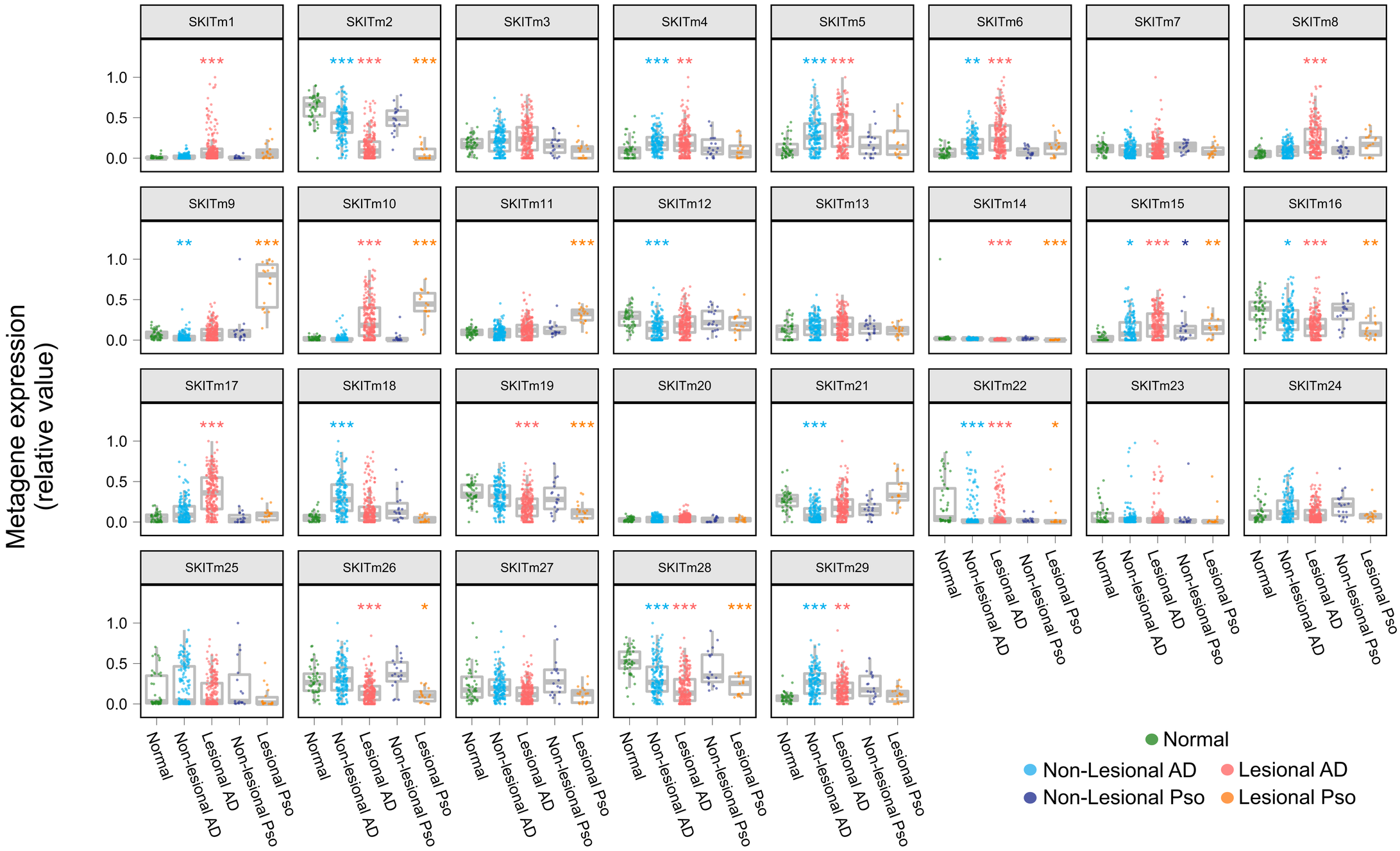

Supplementary Figure 8. Comparison of metagene expression in disease and control samples.

Metagene expression in normal, lesional AD, non-lesional AD, normal, lesional psoriasis, and non-lesional psoriasis samples. The p-values represent the differences in expression compared with normal samples. The Wilcoxon test, corrected with the Bonferroni correction, was used for multiple comparisons. n (samples) = 49 (normal), 246 (lesional AD), 170 (non-lesional AD), 18 (lesional psoriasis), and 18 (non-lesional psoriasis). *p < 0.01, **p < 0.001, *** p < 0.0001.

Supplementary Figure 9.

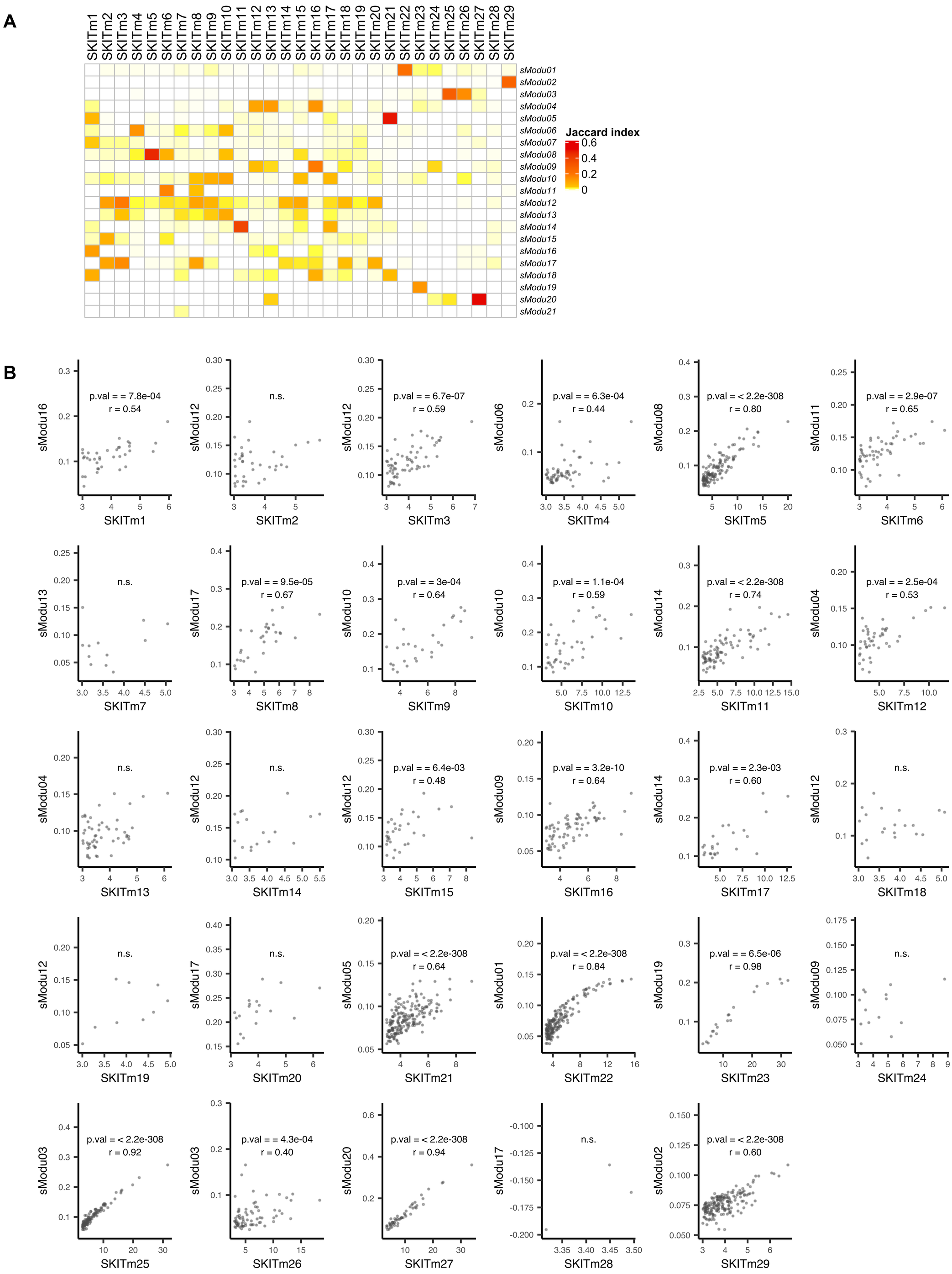

Supplementary Figure 9. Correlation with previously reported skin modules in AD.
A) Heatmap displaying the Jaccard index of the highly-weighted genes in metagenes and contributing genes of skin modules reported in our previous study (Sekita et al., 2023). B) The correlation of weights of common genes included in the skin modules and metagenes. The r and p indicate the correlation coefficient and the significance obtained through Spearman's correlation analysis, respectively. Source data are provided as a Source Data file.

Supplementary Figure 10.

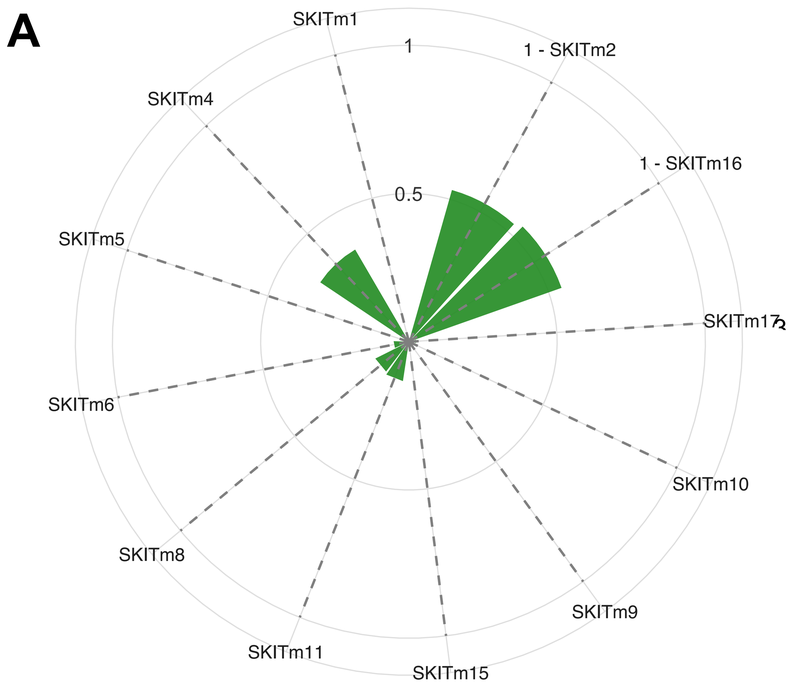

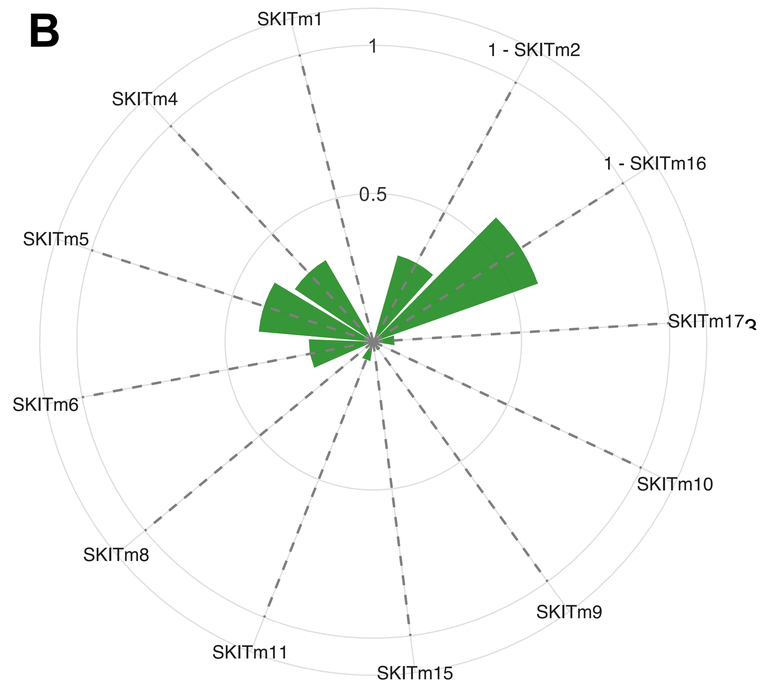

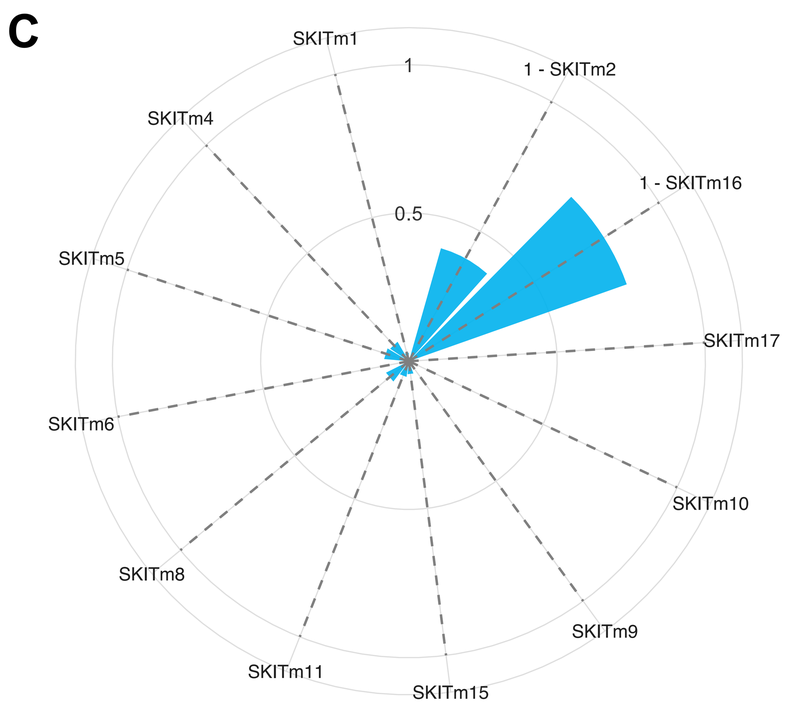

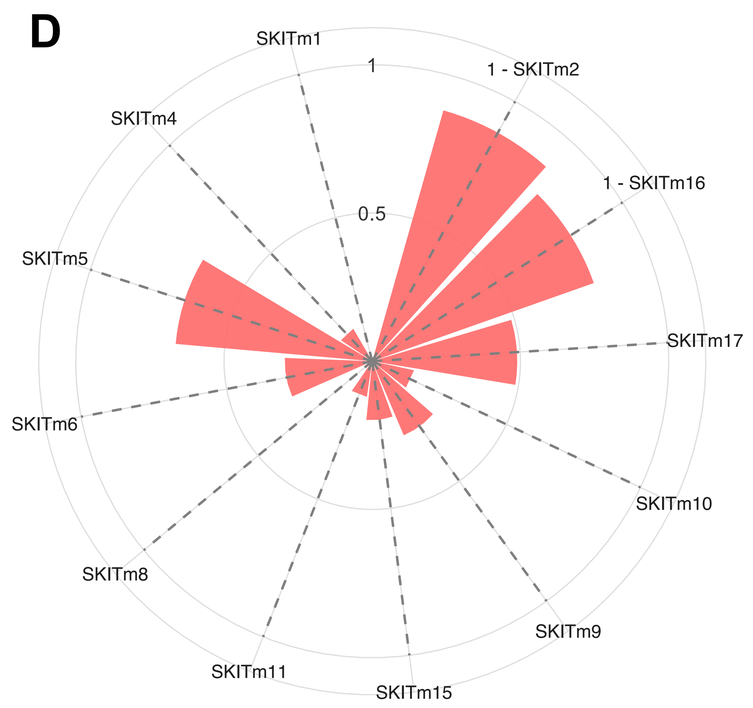

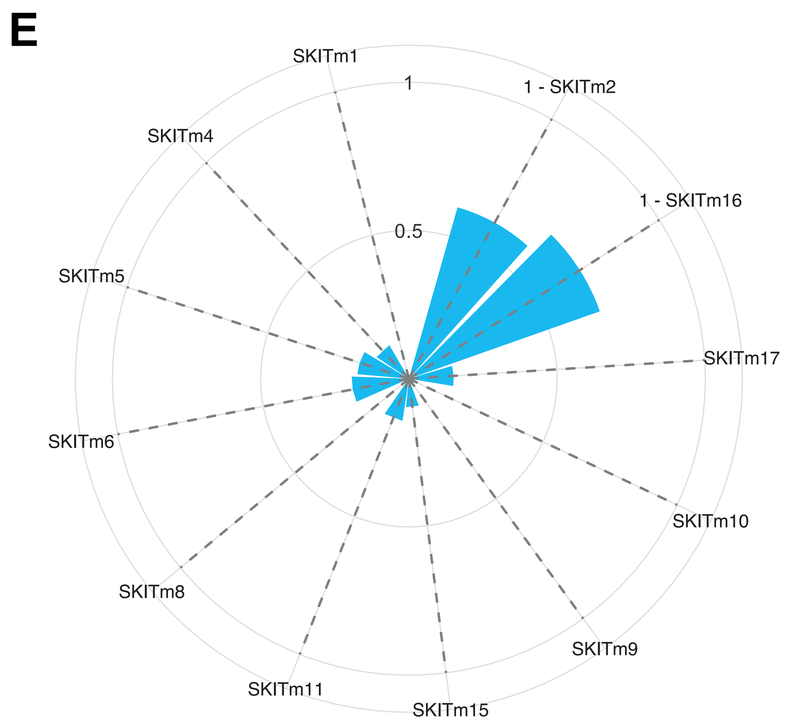

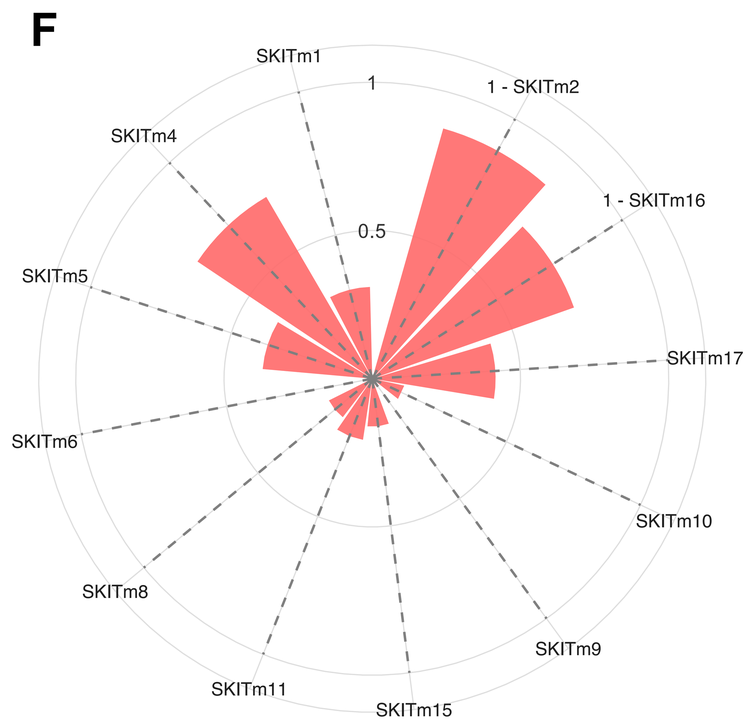

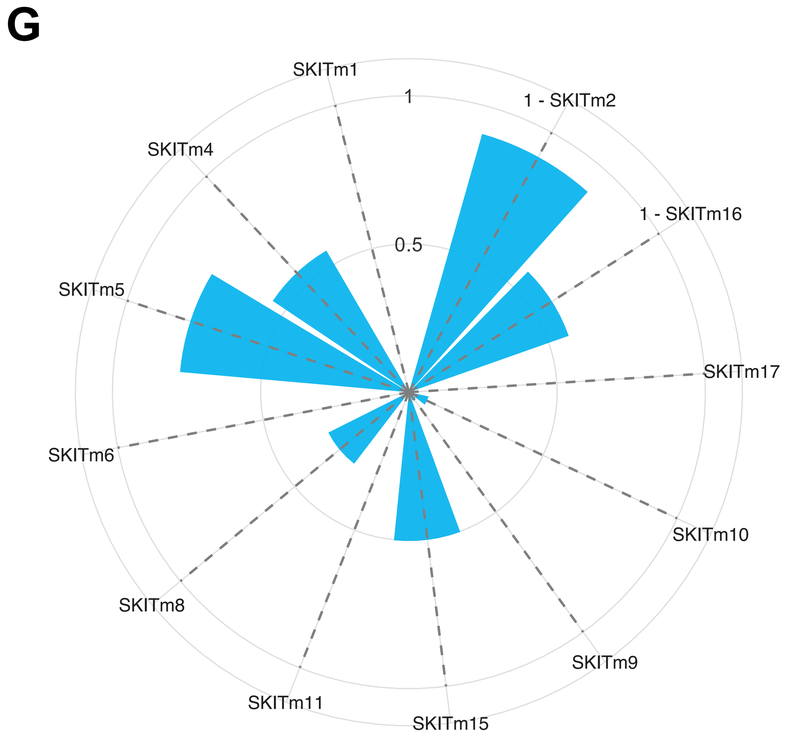

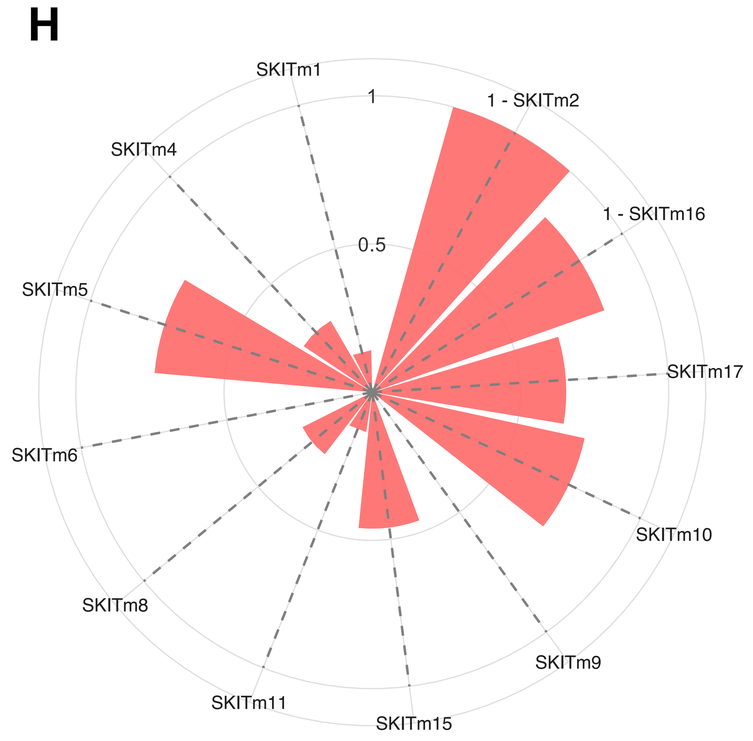

Supplementary Figure 10. Intensity of molecular disruption in each metagene in representative normal and AD subjects.
Circular bar plots visualizing the intensity of molecular disruption in each metagene in representative normal and AD subjects. A) and B) depict normal samples. C) and D represent the non-lesional and lesional samples in an AD subject with mild disease (EASI; 4.4), E) and F) represent the non-lesional and lesional samples in an AD patient with moderate disease (EASI; 18.6), G) and H) represent the non-lesional and lesional samples in an AD patient with severe disease (EASI; 33).

Supplementary Figure 11.

A

Supplementary Figure 11.

Supplementary Figure 11. Regression analysis of skin metagene expression and clinical features.

Each dot represents one sample. The scatter plot shows the fitted regression line with a gray shaded area representing the 95% confidence interval of the predicted values. The *p*-value indicates the significance of the association, as determined by linear regression analysis. A) Analysis of different clinical skin symptoms. The y-axis represents the metagene expression values, and the x-axis denotes the intensity or the presence of skin symptoms. NL: non-lesion; PN: prurigo nodules associated with AD; LA: lichen amyloidosis associated with AD. B) Analysis of disease severity. The y-axis represents the metagene expression values, and the x-axis denotes the intensity of disease severity and pruritus score. Sample sizes: erythema/excoriation/papulation/lichenification (n = 212), LA (n = 12), PN (n = 16), pruritus (lesional, n = 230; non-lesional, n = 151), EASI (lesional, n = 235; non-lesional, n = 159). EASI: Eczema Area and Severity Index. Source data are provided as a Source Data file.

Supplementary Figure 12.

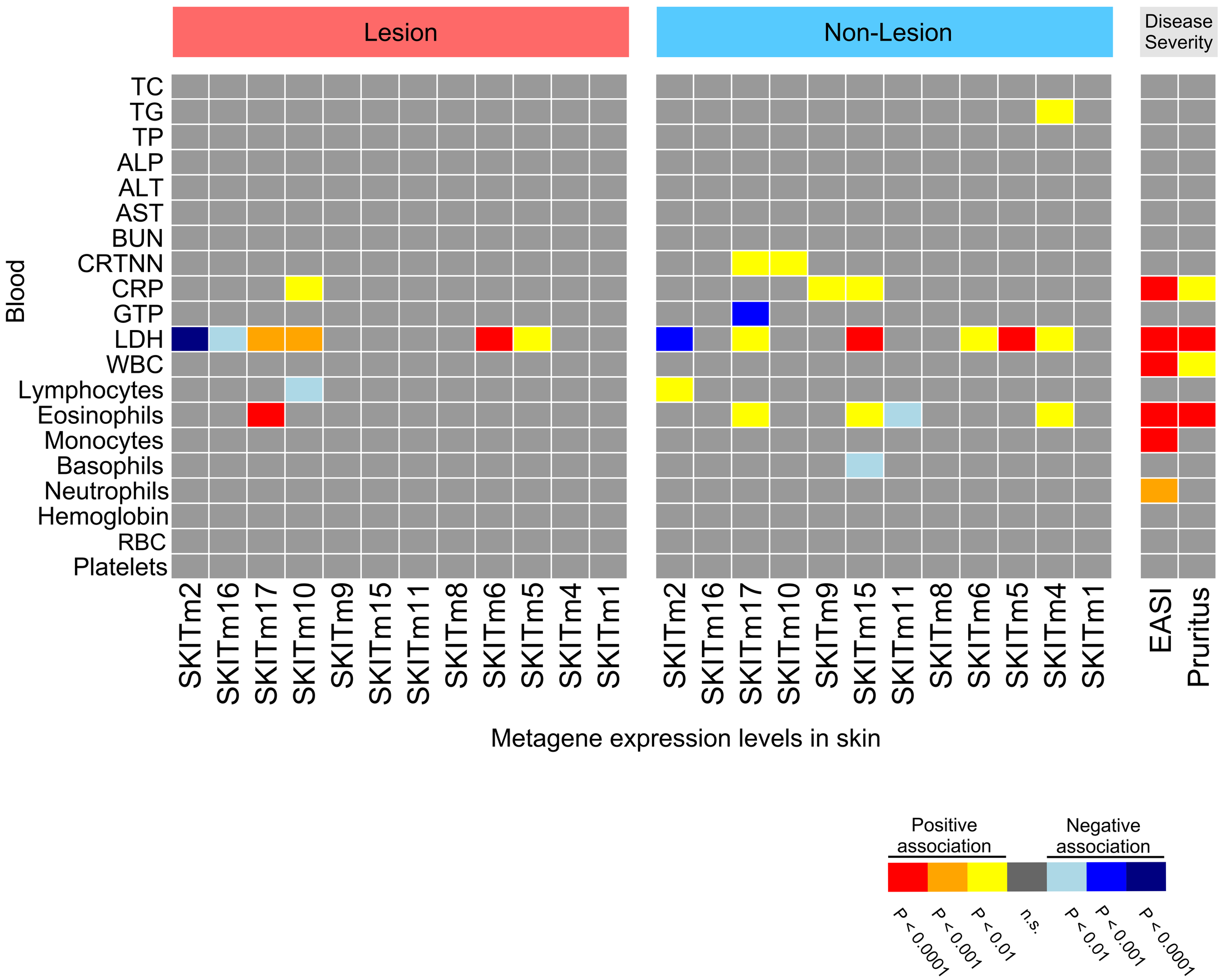

Supplementary Figure 12. Analysis of skin metagene expression and clinical biomarkers in blood.
Heatmap displaying p-values obtained from the regression analysis of skin metagene expression and general clinical parameters of blood samples. Sample sizes: *n* = 205 (lesional), 139 (non-lesional) for most parameters; ALP (181/124), LDH (203/137), basophils (201/136), neutrophils (195/135), and TC/TG (202/136). TB, total bilirubin; TC: total cholesterol; TG: triglycerides, TP: total protein; ALP, alkaline phosphatase; ALT, alanine aminotransferase; AST, aspartate aminotransferase; BUN, blood urea nitrogen; CRTNN, C-reactive protein; GTP, gamma-glutamyl transferase; LDH, lactate dehydrogenase; WBC, white blood cells; RBC, red blood cells. Source data are provided as a Source Data file.

Supplementary Figure 13.

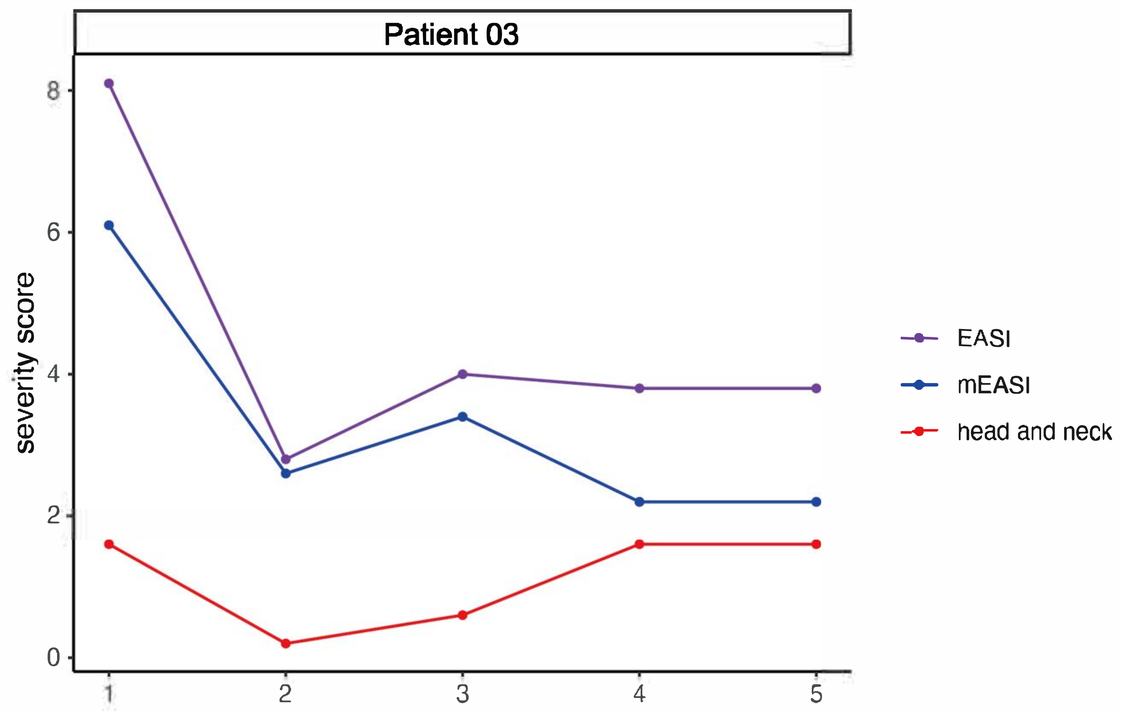

3 months

4 months

Supplementary Figure 13. A representative case of dupilumab-associated facial erythema.
Clinical photograph of Patient 03 exhibiting dupilumab-associated facial erythema (DFE) during the longitudinal study. The patient developed non-pruritic erythema across the entire face after 4 months of dupilumab treatment, while the pre-existing skin symptoms of AD on the trunk and extremities showed improvement. Only the right cheek of the face is presented for privacy reasons.

Supplementary Figure 14.

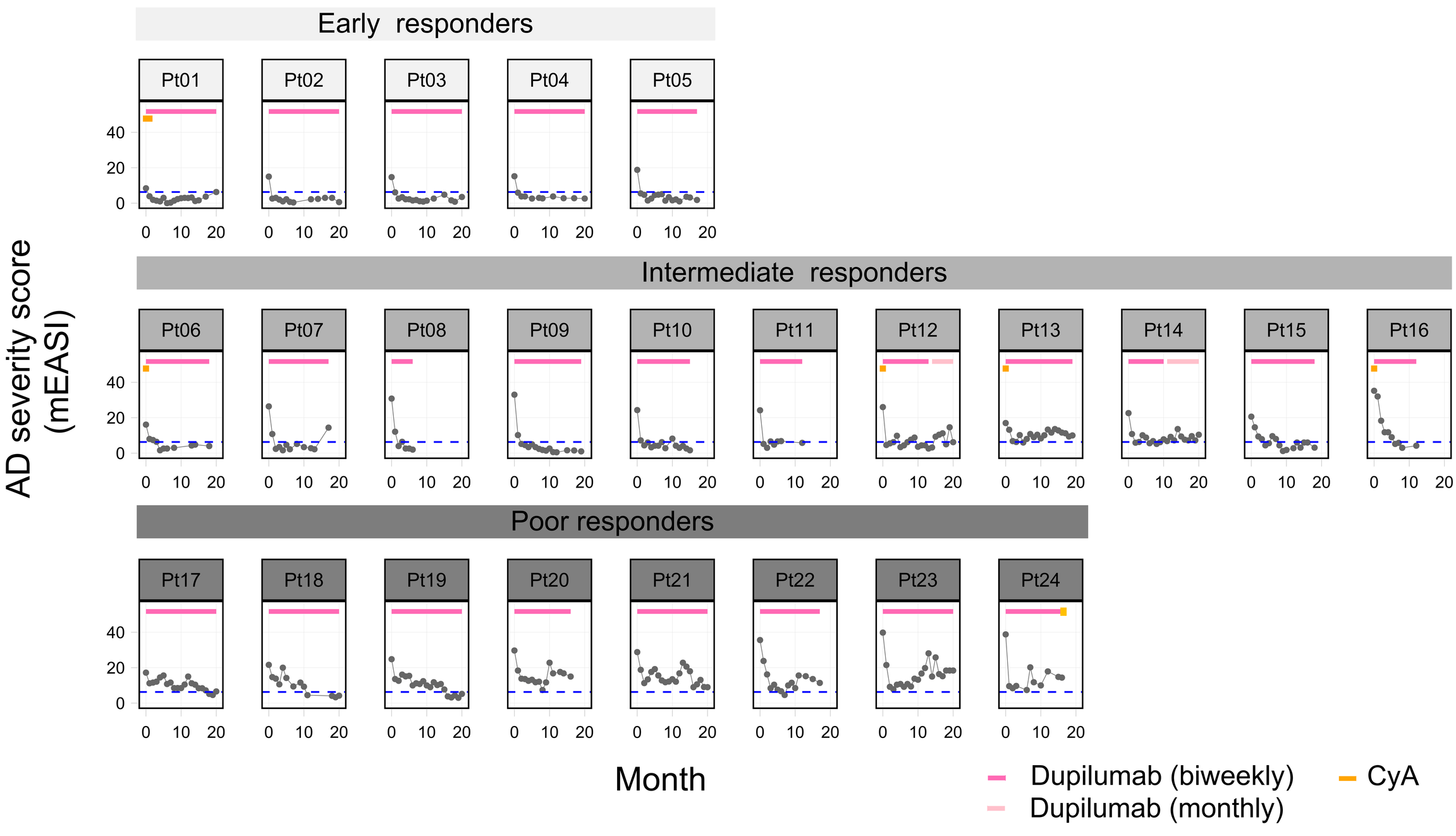

Supplementary Figure 14. Longitudinal analysis of patients treated with dupilumab. Time-course of disease severity (modified Eczema Area and Severity Index: mEASI) in patients treated with dupilumab. The blue line represents 6.3, which is the cutoff for mild disease severity in the mEASI. Responder groups were based on the mEASI during the first 6 months of dupilumab treatment. Dark and light pink lines indicate that patients were administered dupilumab biweekly and monthly, respectively. The orange line indicates patients who received oral cyclosporine.

Supplementary Figure 15.

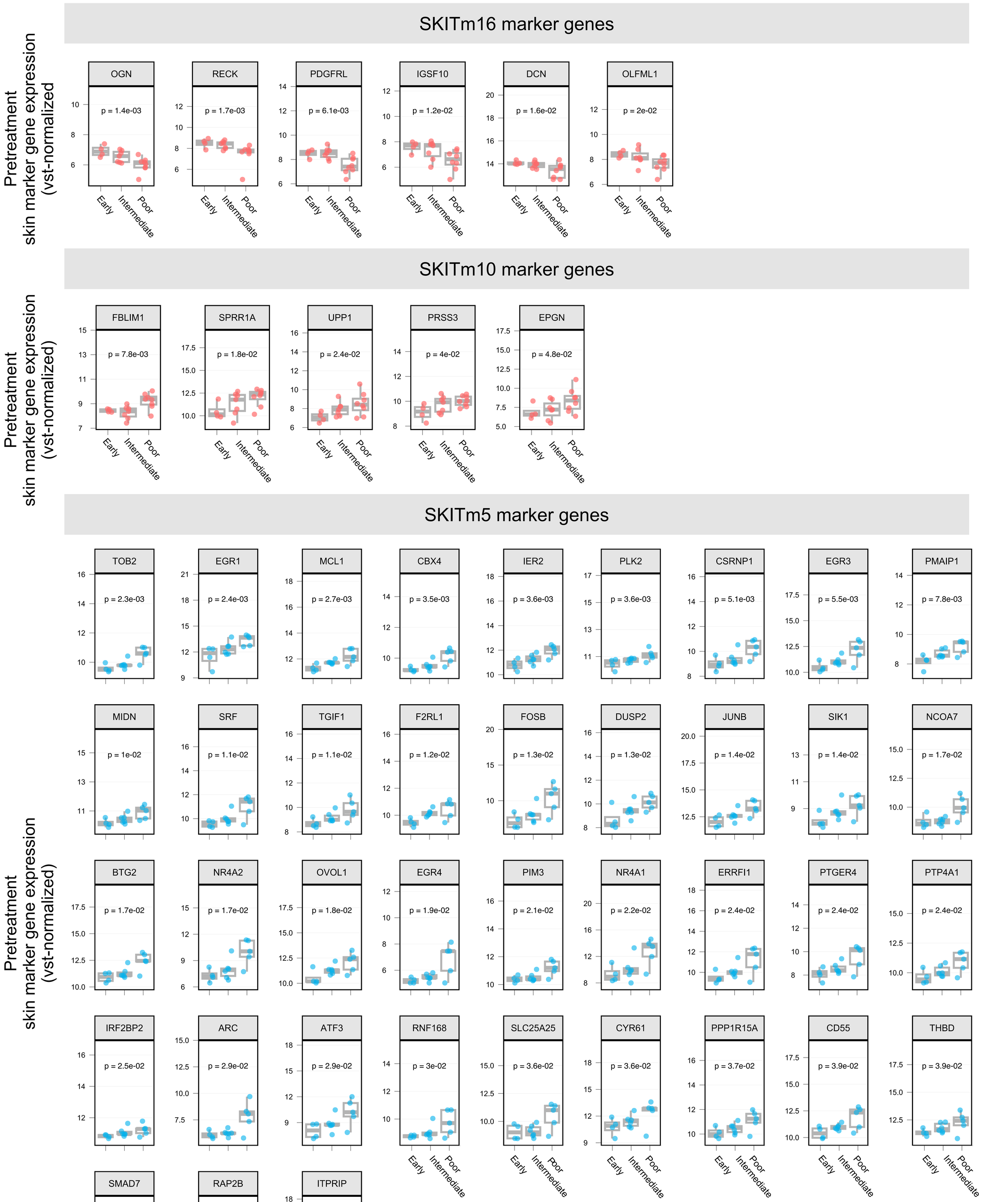

Supplementary Figure 15. Correlation between pretreatment expression levels of marker genes and dupilumab treatment outcomes.
Genes with p-values < 0.05 are presented. The p-values indicate the significance obtained through Spearman's correlation analysis. n (samples) = 19 (lesional AD skin), 15 (non-lesional AD skin). Source data are provided as a Source Data file.

Supplementary Figure 16.

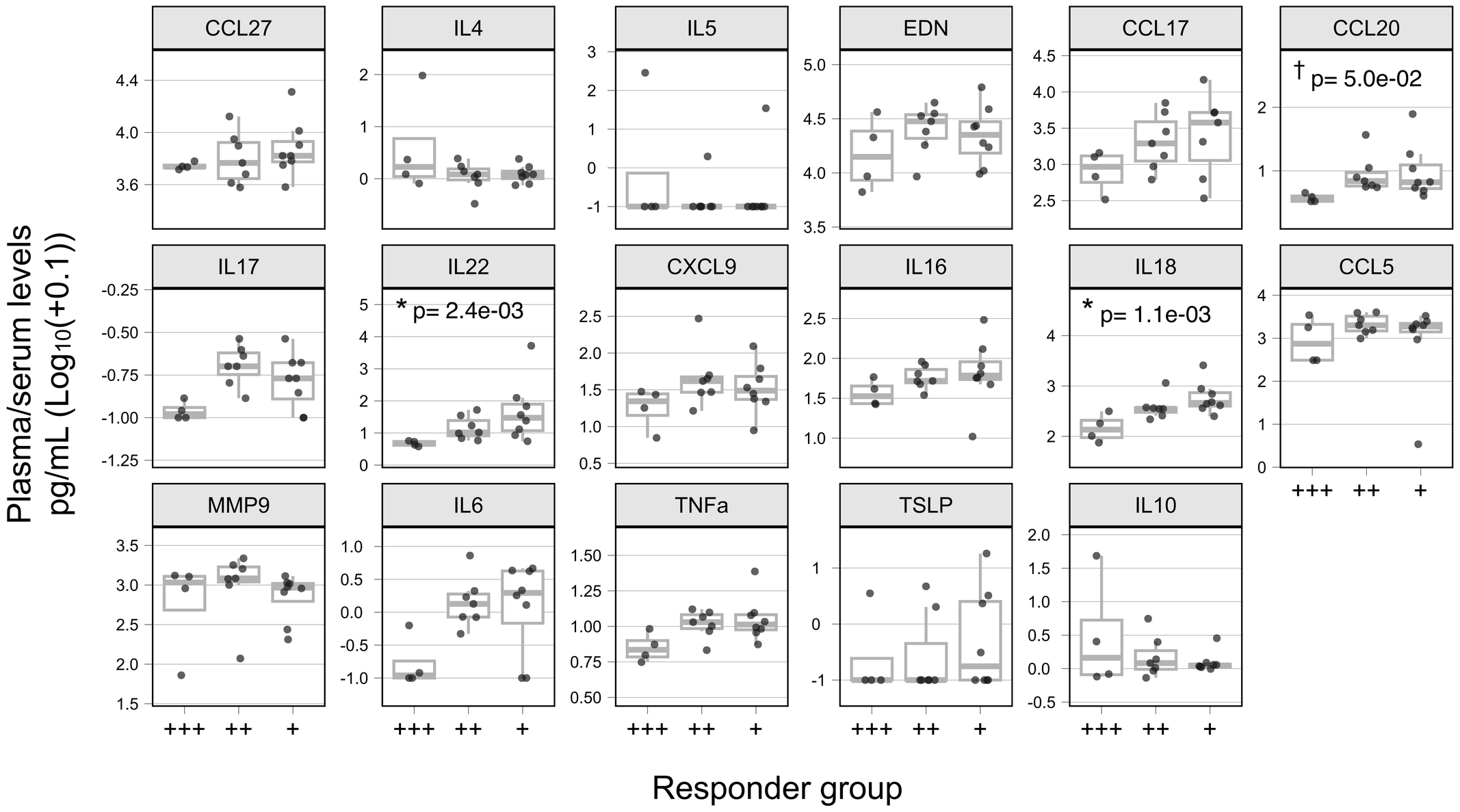

Supplementary Figure 16. Correlation between pretreatment blood cytokine levels and dupilumab treatment outcomes.
The p-values indicate the significance obtained through Spearman's correlation analysis. Responder groups are categorized as follows: **+++** (early responder), **++** (intermediate responder), **+** (poor responder). n = 19. *p < 0.01, †p < 0.05. Source data are provided as a Source Data file.

Supplementary Figure 17.

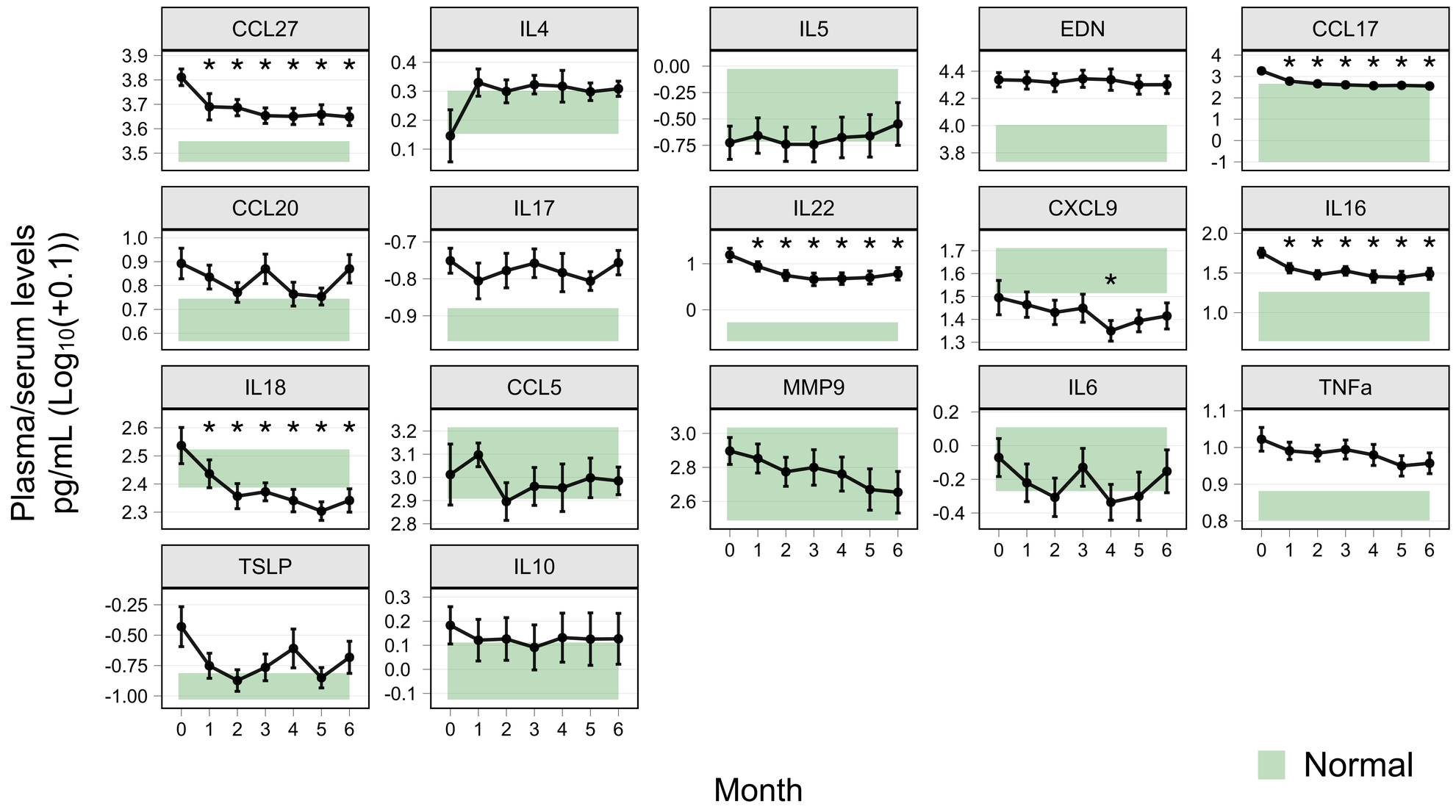

Supplementary Figure 17. Average transition in blood cytokines during dupilumab treatment in 24 patients.
The p-values indicate the difference in blood cytokine levels compared with that at the baseline. The error bars represent the standard error of the mean (SEM). Green highlighted shadows represent the 95% CI of the mean expression levels in healthy individuals. P-values were corrected using the Bonferroni method for multiple comparisons. n = 24. *p < 0.01. Source data are provided as a Source Data file.

Supplementary Figure 18.

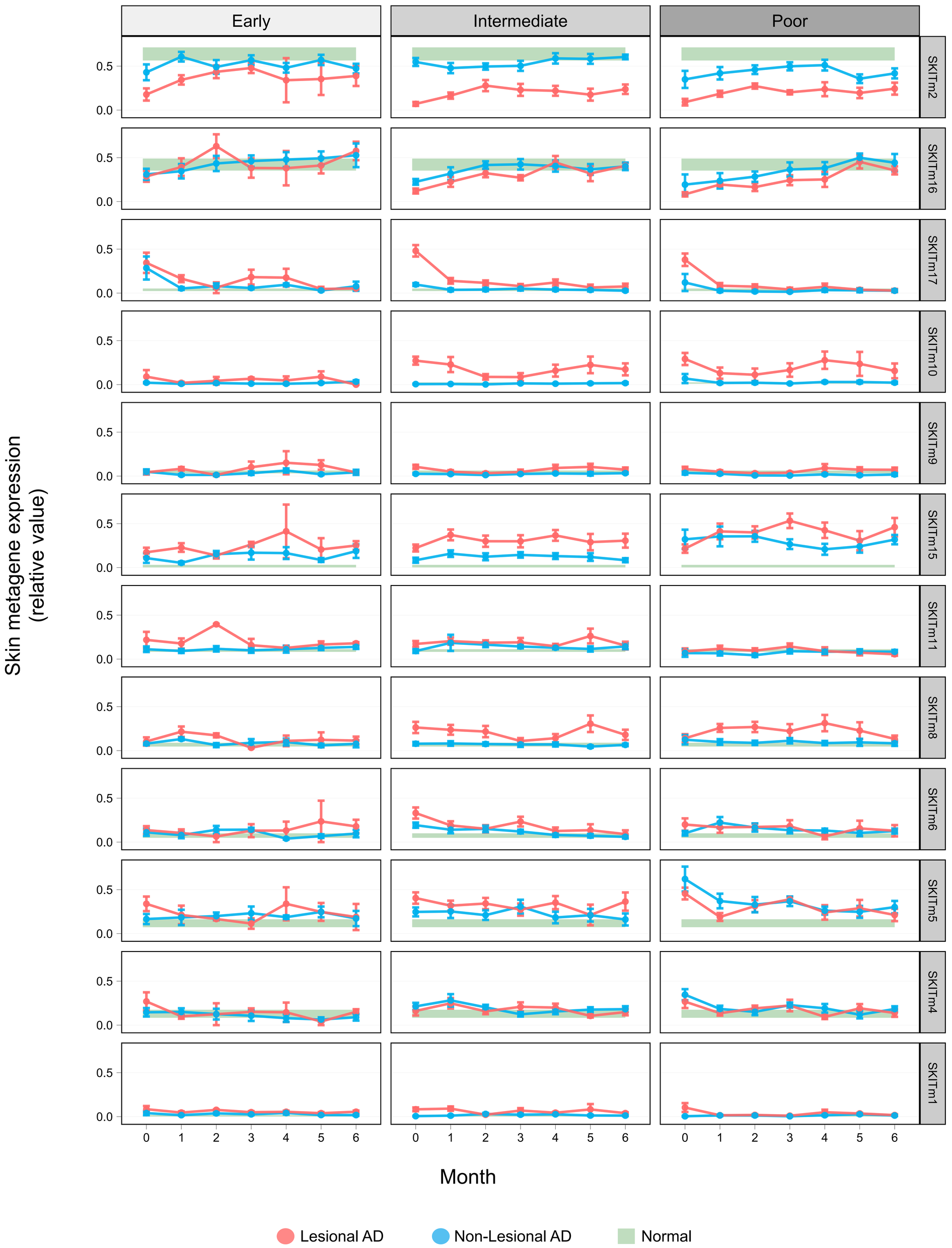

Supplementary Figure 18. Average transition in skin metagene expression in different responder groups.
The mean and SEM are depicted as red and blue points and bars, respectively, for lesional and non-lesional AD skin samples. Green highlighted shadows represent the 95% CI for the mean expression in healthy individuals. n = 5 (early responders), 11 (intermediate responders), 8 (poor responders).

Supplementary Figure 19.

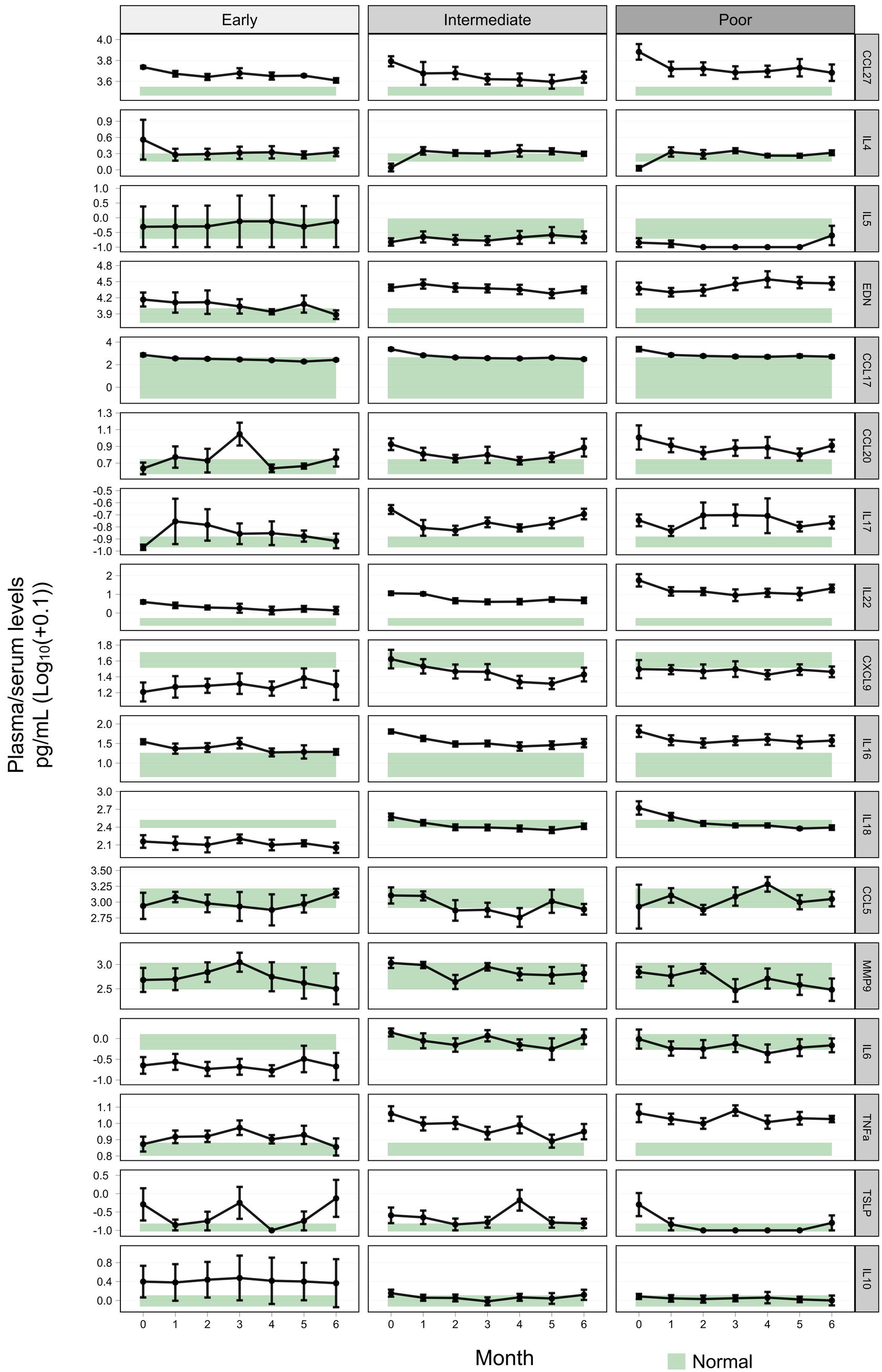

Supplementary Figure 19. Average transition in blood cytokine levels in different responder groups.
The error bars represent the standard error of the mean (SEM). Green highlighted shadows represent the 95% CI for the mean expression in healthy individuals. Samples from 24 patients were analyzed.

Supplementary Figure 20.

Supplementary Figure 20. Dynamics of skin metagene expression in individual patients over a long course of dupilumab treatment.
Green highlighted shadows represent the 95% CI for the mean expression in healthy individuals. Samples from eight patients were analyzed.

Supplementary Figure 21.

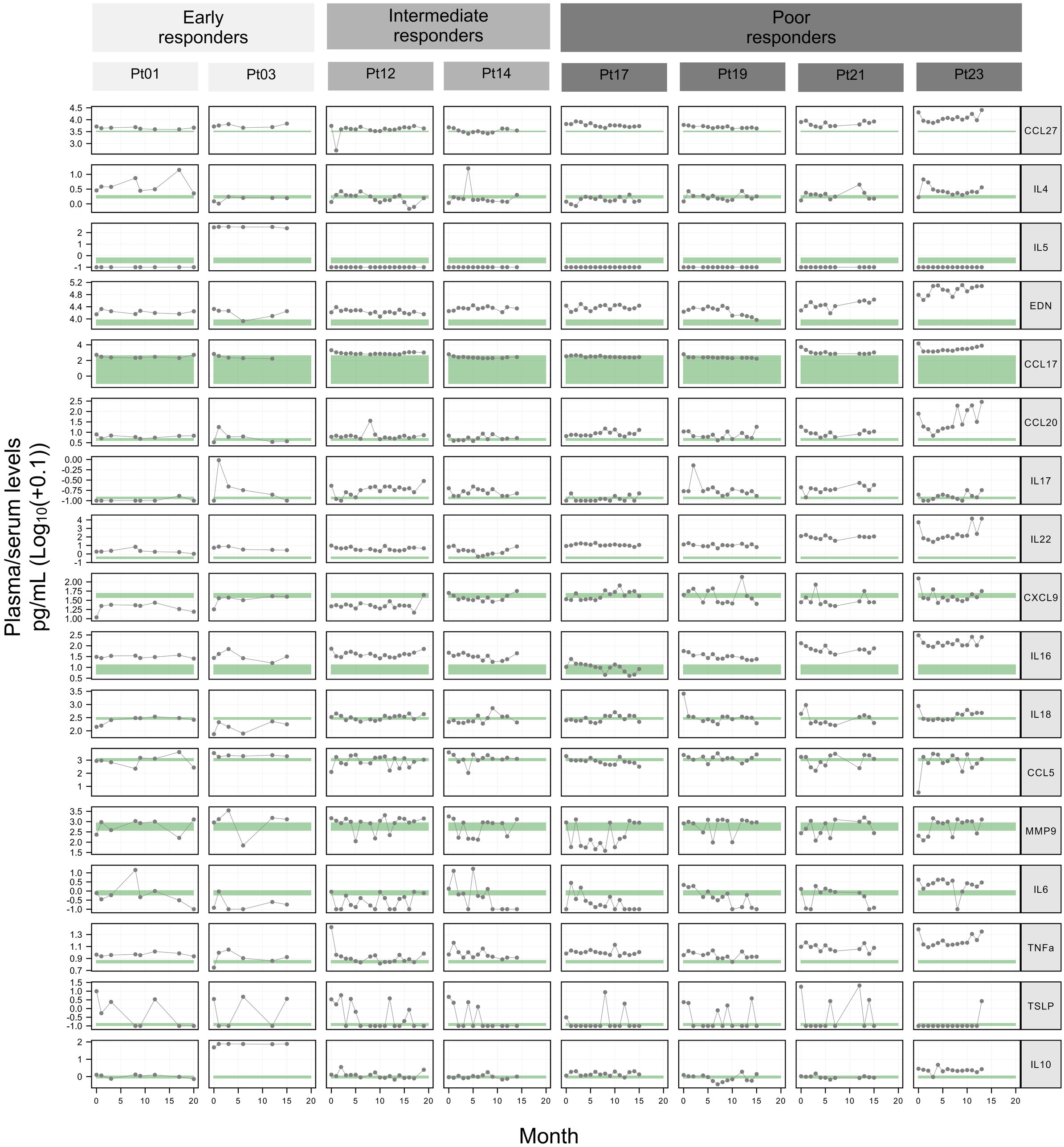

Supplementary Figure 21. Dynamics of blood cytokine levels in individual patients during long-course dupilumab treatment.
Green highlighted shadows represent the 95% CI for the mean expression in healthy individuals.

Supplementary Figure 22.

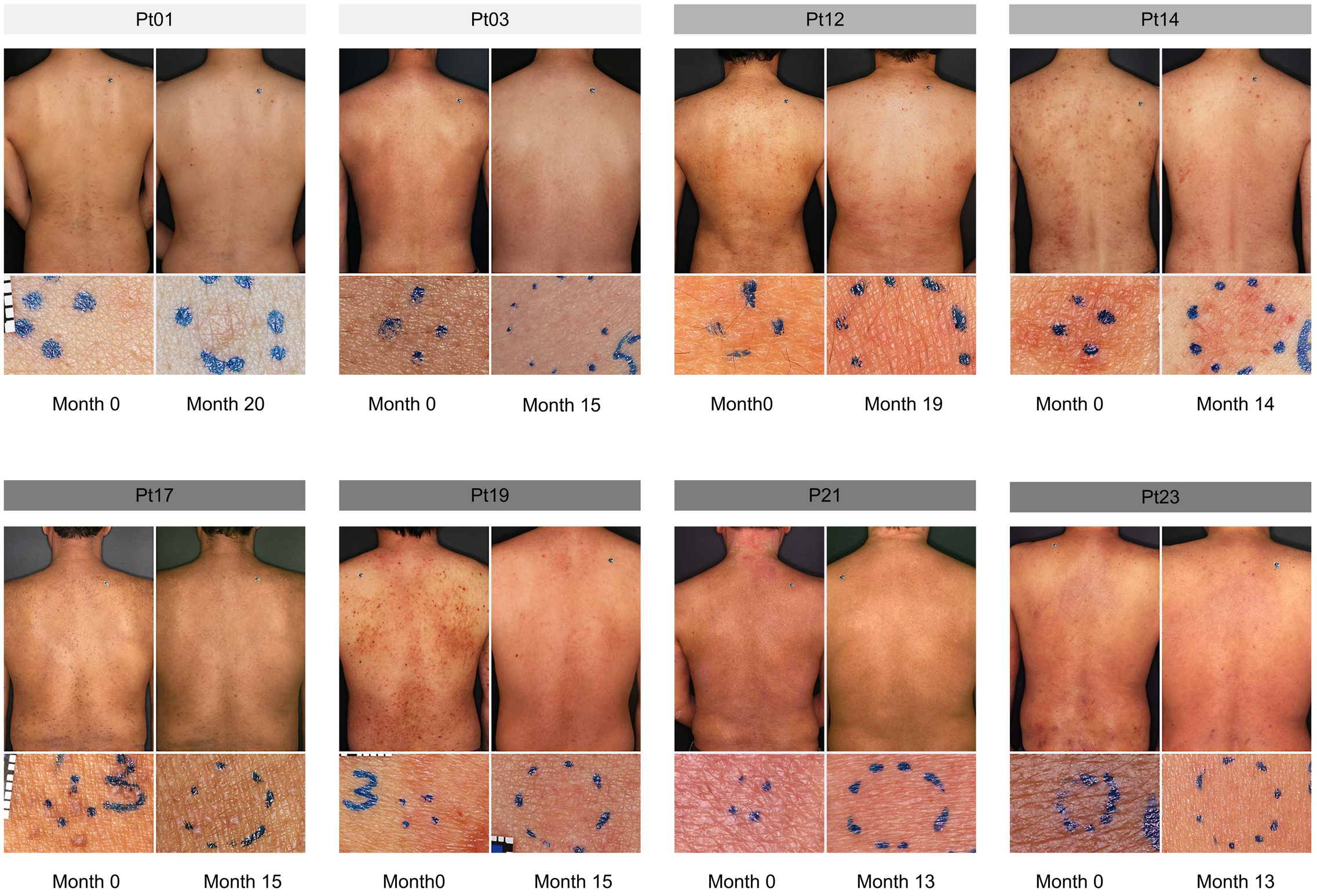

Supplementary Figure 22. Clinical images of the patients analyzed in Figure 5C and 5D. The upper and lower parts of each image depict the upper trunk and sampled region, respectively. The 1-mm skin samples were obtained from the circled areas.

Supplementary Figure 23.

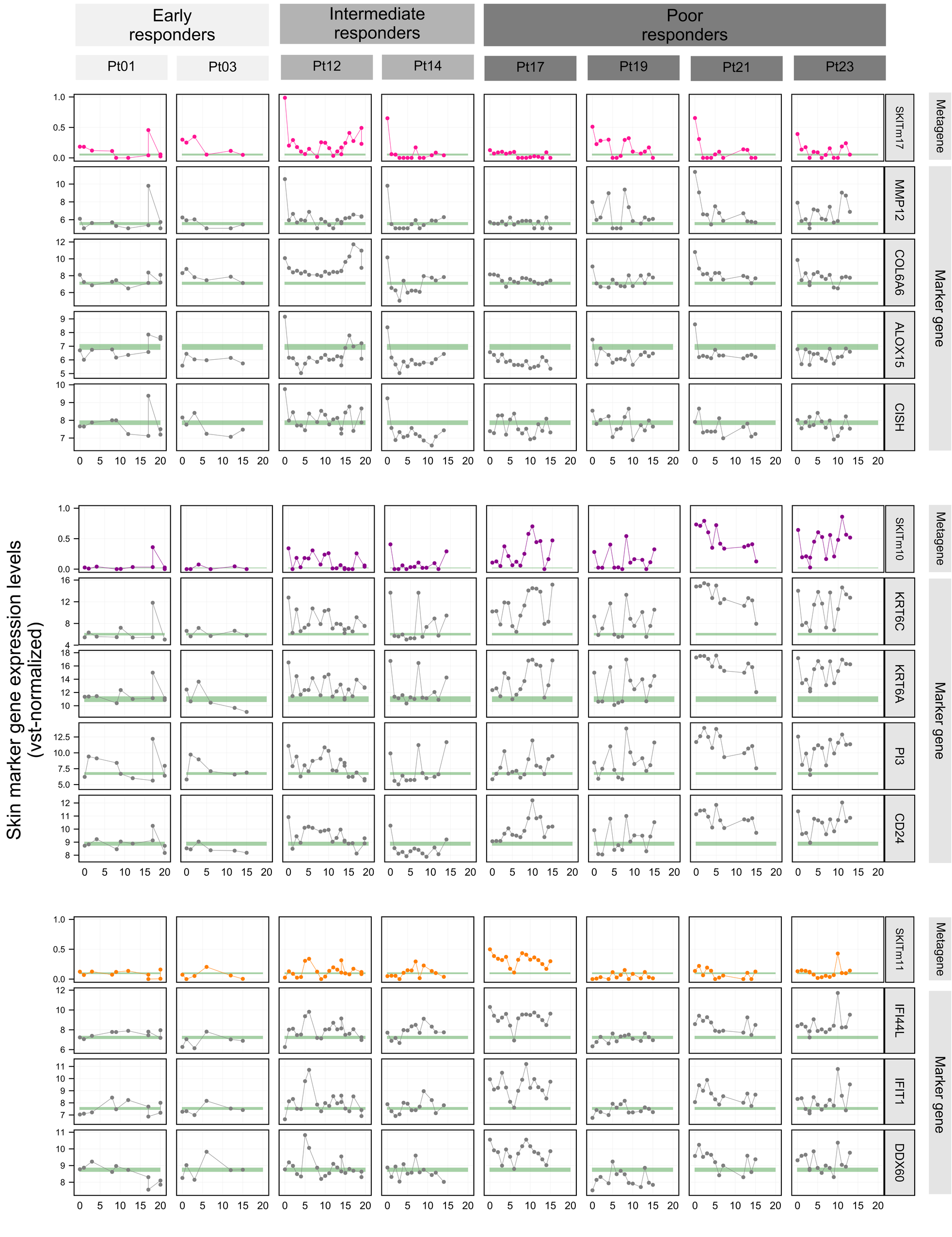

Supplementary Figure 23.

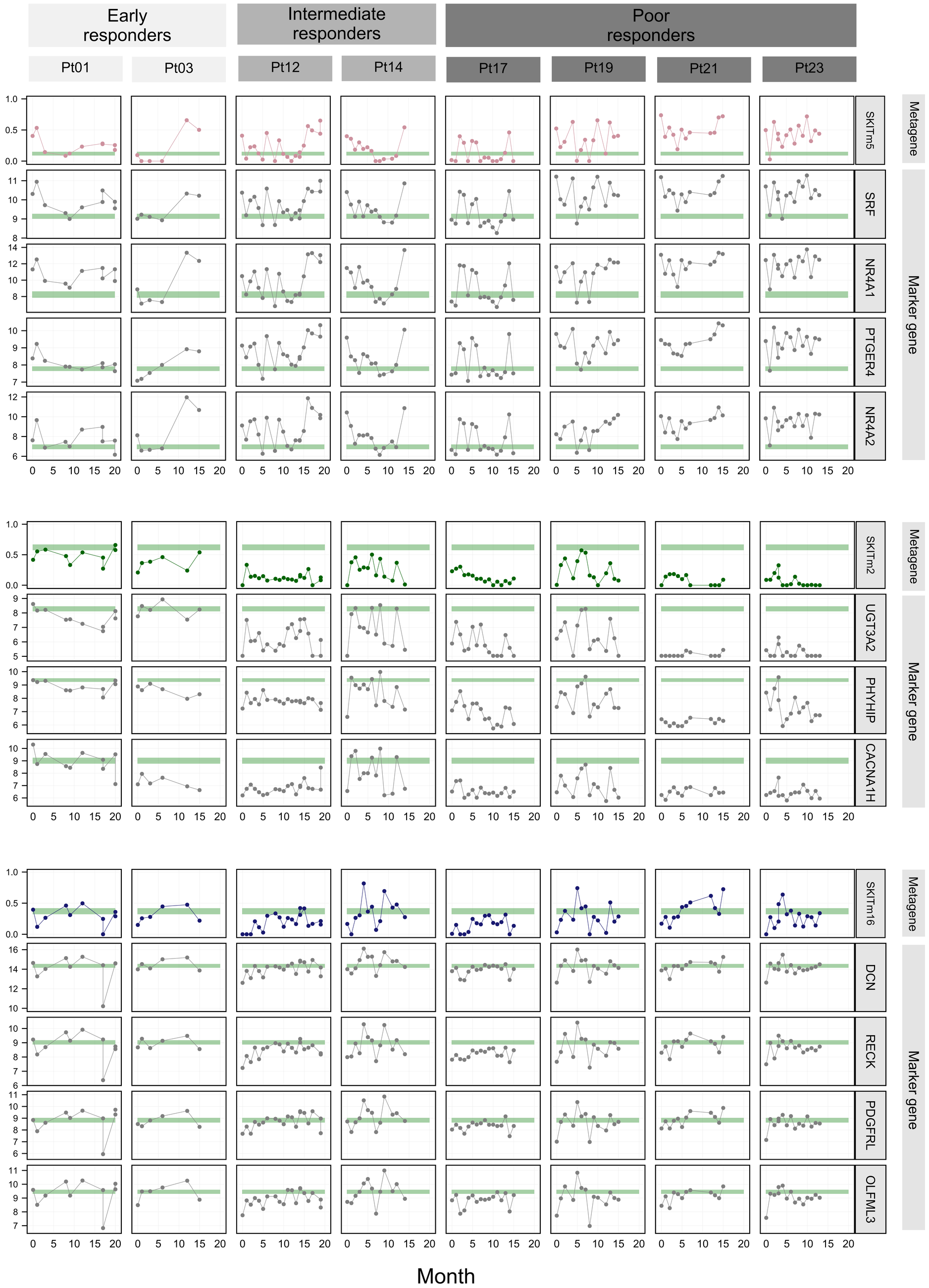

Supplementary Figure 23. Metagene expression and marker gene expression dynamics in lesional samples during long-course dupilumab treatment.
The sequential dynamics of metagene expression and the top five correlated marker genes are displayed. Marker gene expression is presented as variance-stabilizing transformation (vst)-normalized values. Green highlighted shadows represent the 95% CI for the mean expression in healthy individuals.

Supplementary Figure 24.

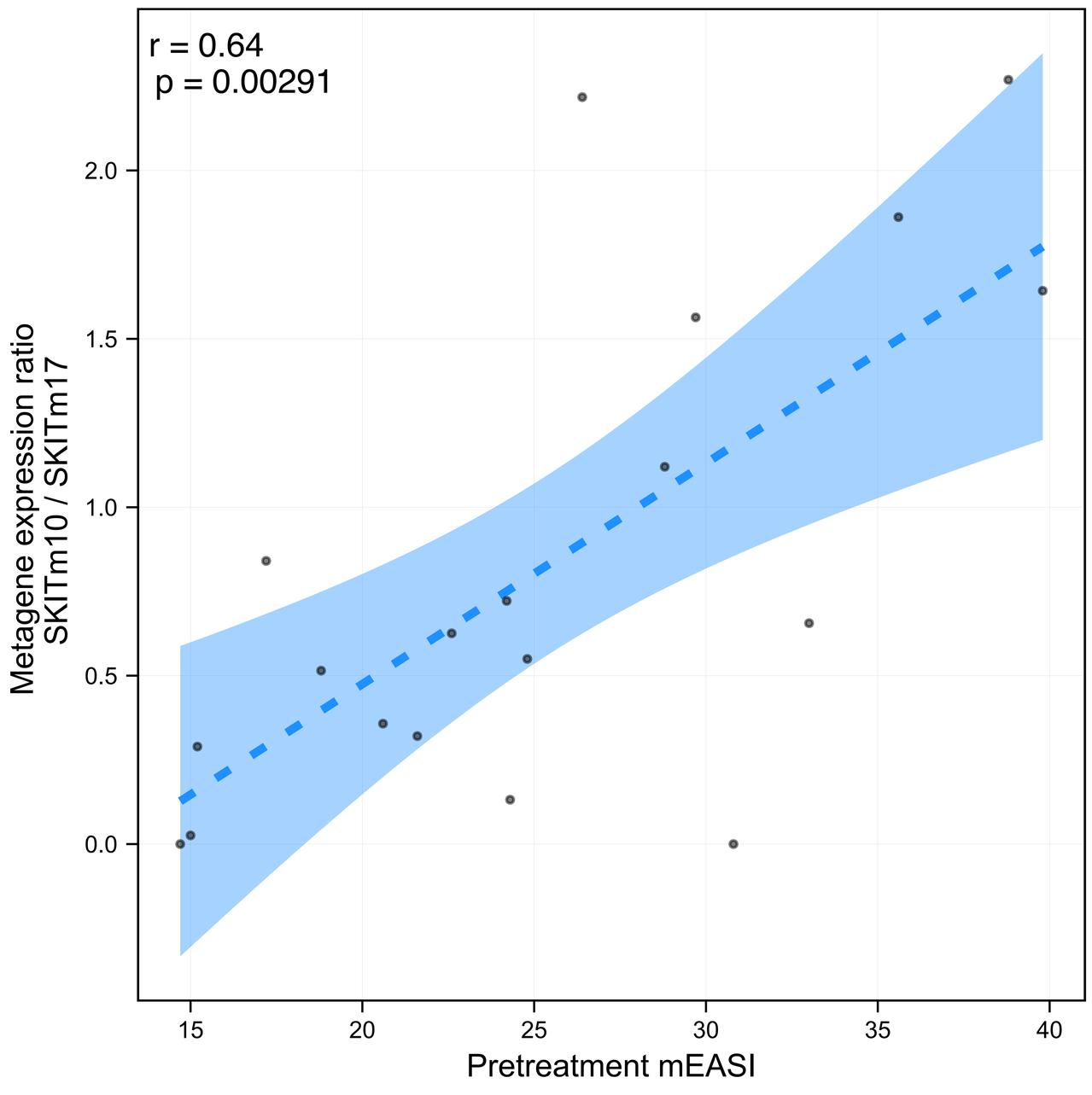

Supplementary Figure 24. Correlation of SKITm10/SKITm17 expression and disease severity before dupilumab treatment.
The y-axis represents the ratio of SKITm10 expression over SKITm17 expression, and the x-axis represents the severity score before initiating dupilumab treatment, The r and p indicate the correlation coefficient and the significance obtained through Spearman's correlation analysis, respectively. n = 19 samples. Source data are provided as a Source Data file.

Supplementary Figure 25.

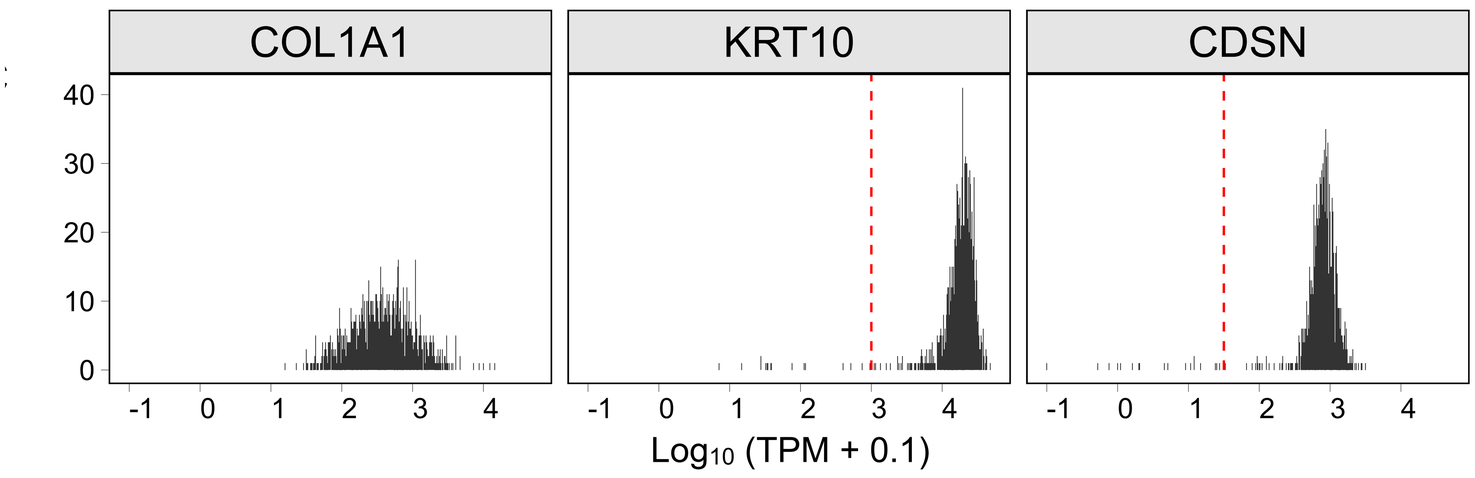

Supplementary Figure 25. Distribution of representative structural genes used for assessing the adequate inclusion of dermis and epidermis in the samples.
C) The inclusion of the dermis was assessed based on *COL1A1* as a representative gene in fibroblasts, and the inclusion of the spinous layer and stratum corneum was assessed based on *KRT10* and *CDSN*, respectively. Red dashed lines indicate the cutoff for sample filtering. n = 1061 samples.

Supplementary Figure 26.

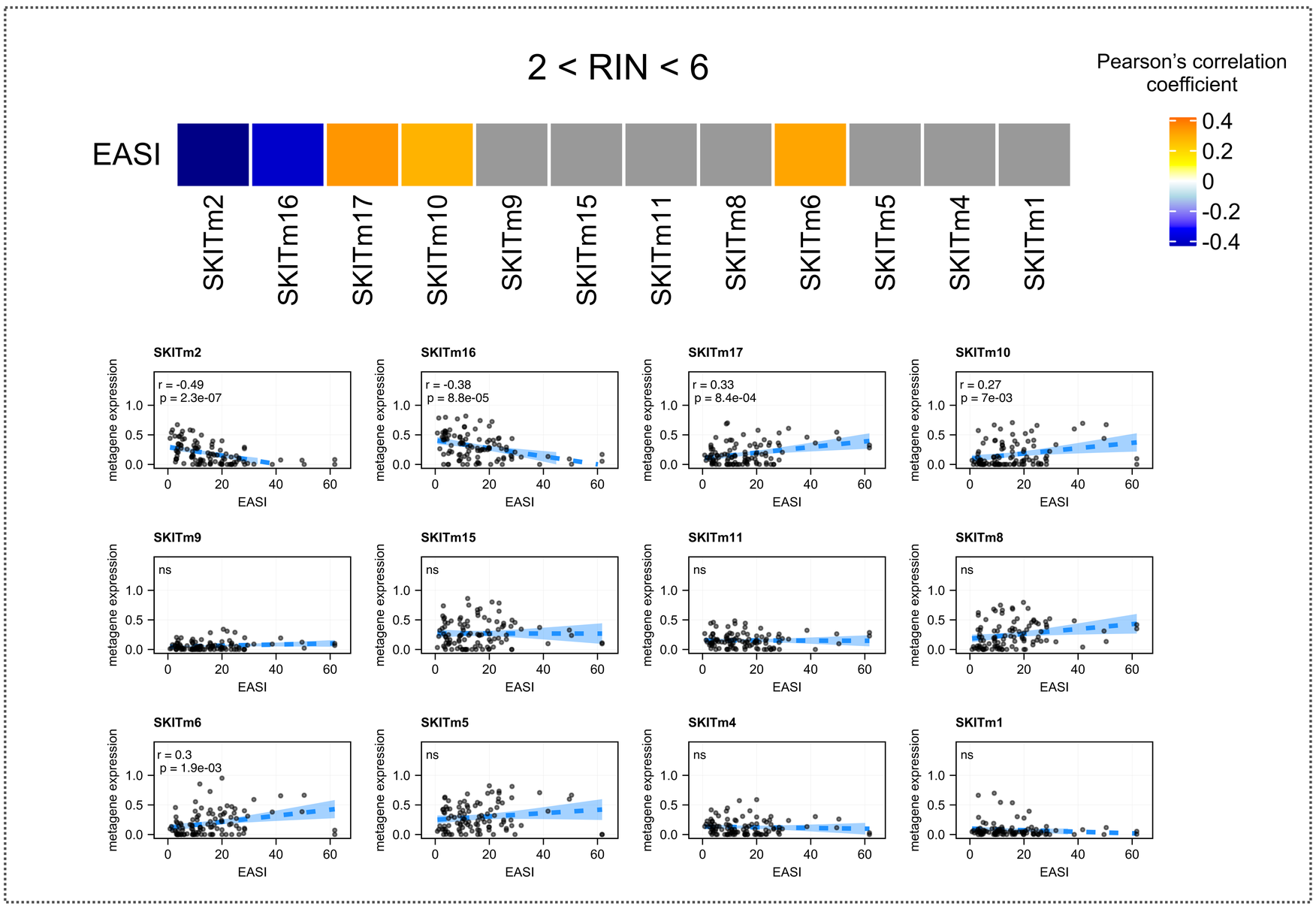

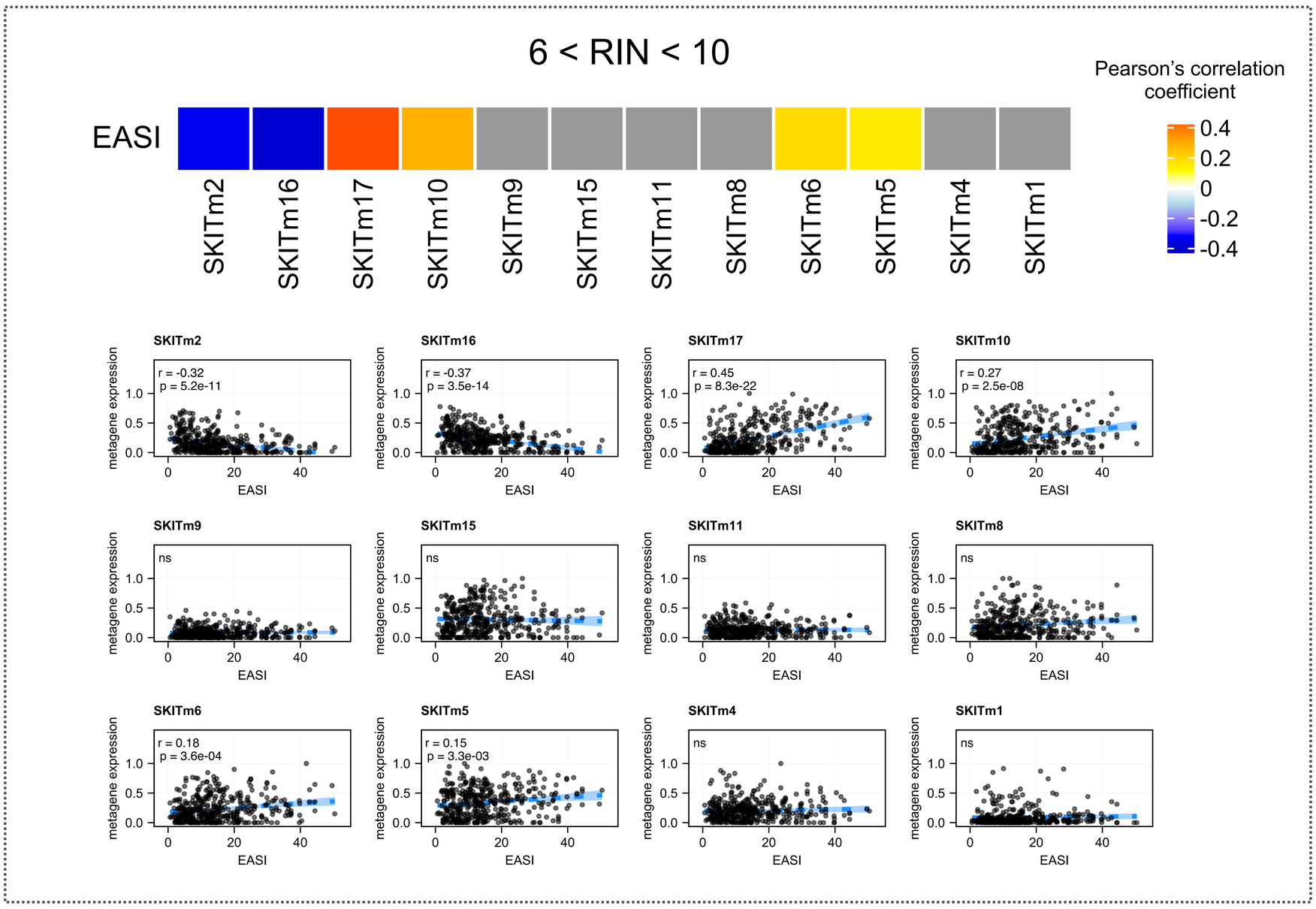

Supplementary Figure 26. Correlation analysis of disease severity and meta genes stratified by RIN score.
Correlation analysis of disease severity (EASI) and metagene expression in AD samples, stratified by RIN scores of the samples (<6 and ≥6). The heatmap displays Pearson's correlation coefficients, where blue indicates significant negative correlations and red indicates significant positive correlations ($p < 0.01$). Insignificant results are presented in gray. The r and p presented in the scatterplots indicate the correlation coefficient and the significance obtained through Pearson's correlation analysis, respectively. The linear regression line and the 95% CI (shown by blue shadow) are presented. Source data are provided as a Source Data file.

Supplementary Figure 27.

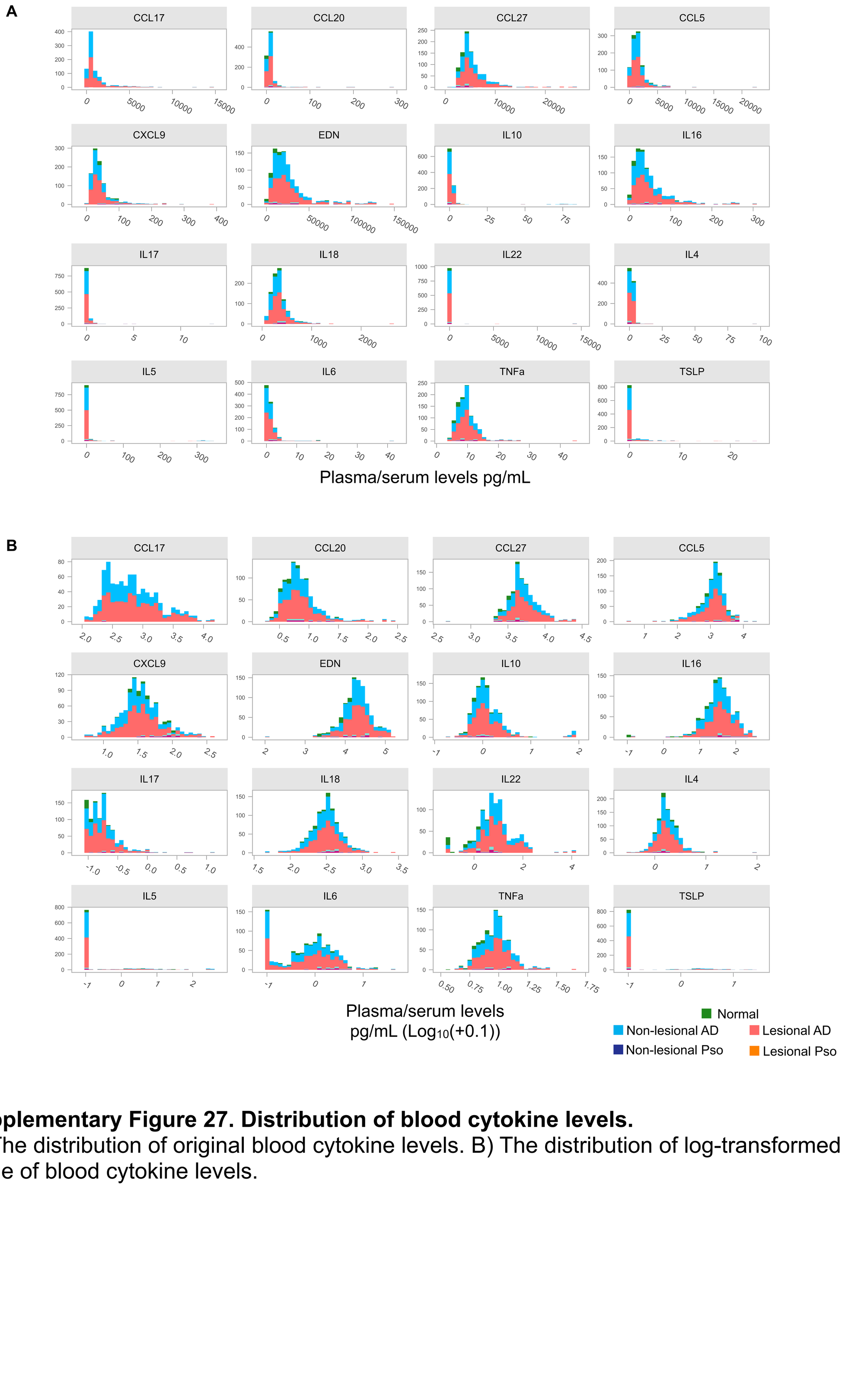

Supplementary Figure 27. Distribution of blood cytokine levels.
A) The distribution of original blood cytokine levels. B) The distribution of log-transformed value of blood cytokine levels.

Supplementary Figure 28.

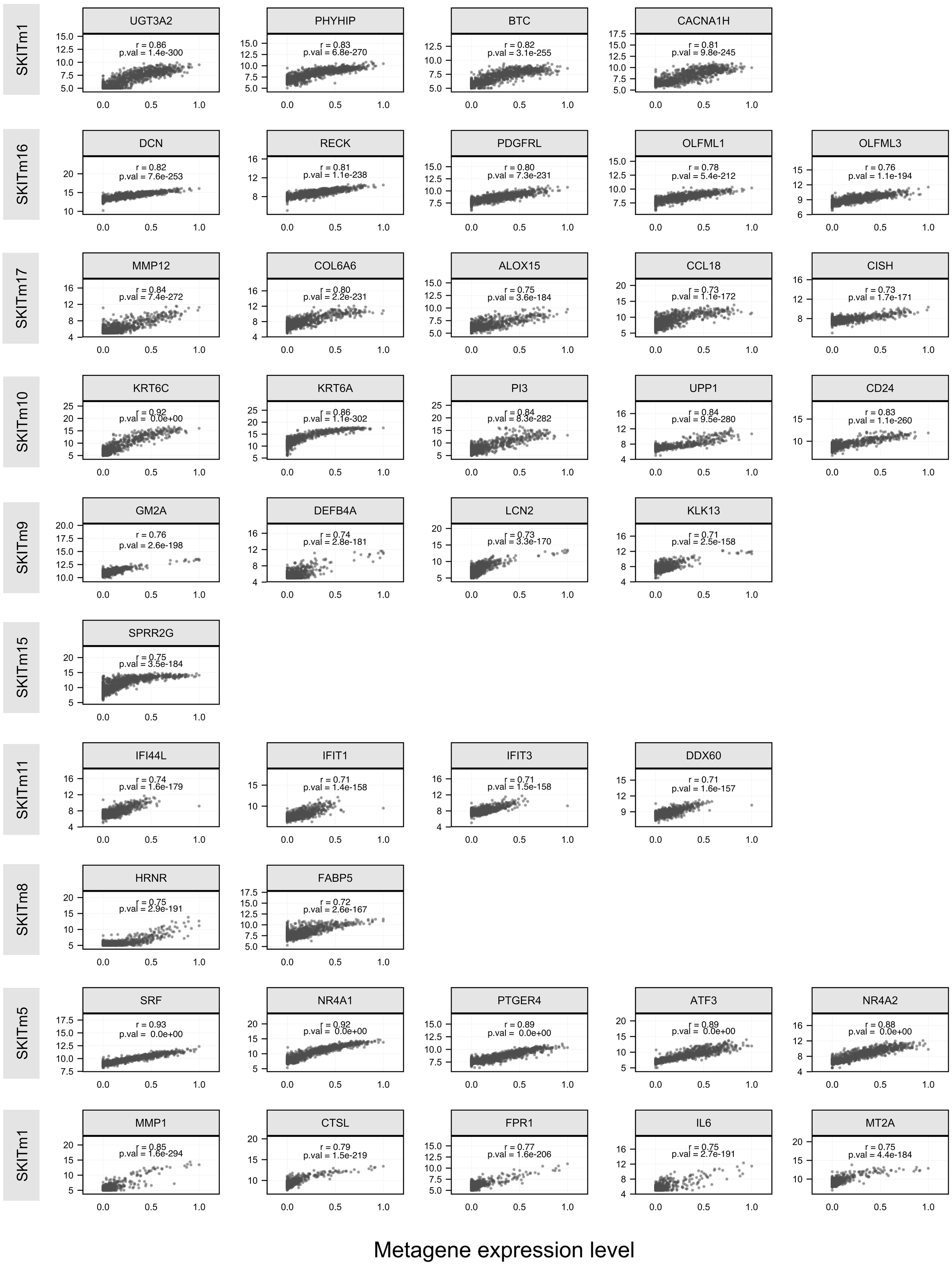

Supplementary Figure 28. Marker genes of the metagenes.
Correlation between metagene expression and variance-stabilizing transformation (vst) expression of marker genes. Each dot represents a single sample. The genes are presented from left to right in order of the lowest p-values in the Pearson's correlation test. For metagenes with more than five marker genes, only the top five genes with the lowest p-values are depicted. n (samples) = 49 (normal), 529 (lesional AD), 422 (non-lesional AD), 18 (lesional psoriasis), and 18 (non-lesional psoriasis). Source data are provided as a Source Data file.

Supplementary Figure 29.

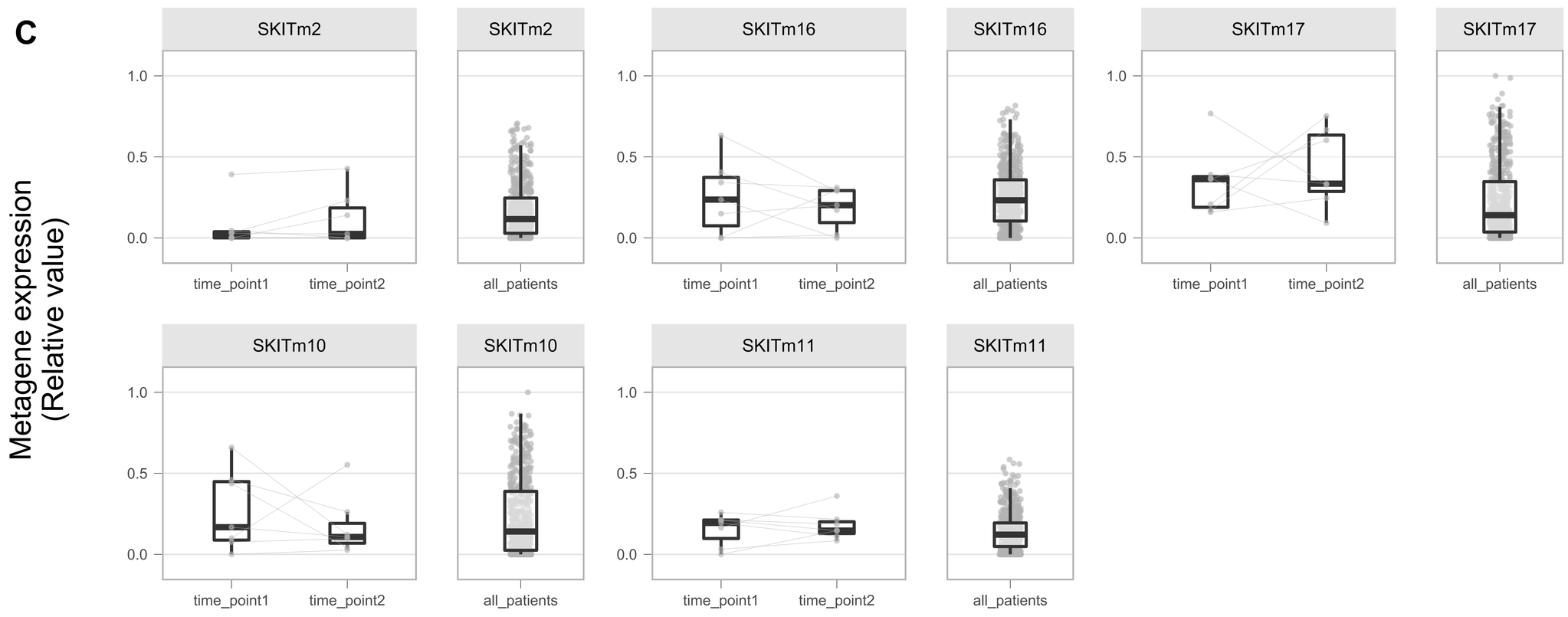

Supplementary Figure 29. Transcriptional profiles of samples with the same local severity obtained from the same patient at different time points.
The transcriptional profiles of samples with the same local severity obtained from the same patient at different time points (n = 7 AD patients). The left column panel represents the skin metagene expression sampled on different dates from lesions of the same patient with the same local severity. The right panel represents the distribution of skin metagene expression in all the lesions of AD patients. The metagene expressions of samples obtained at different time points exhibited no statistical significance.

Supplementary Table 1.

Disease	Lesion / Non-Lesion	Region	Number of samples
AD	Lesion	trunk	467
AD	Lesion	arm	1
AD	Lesion	neck	59
AD	Lesion	face	2
AD	Non-Lesion	trunk	411
AD	Non-Lesion	neck	10
AD	Non-Lesion	face	1
Psoriasis	Lesion	trunk	16
Psoriasis	Lesion	arm	2
Psoriasis	Non-Lesion	trunk	16
Psoriasis	Non-Lesion	arm	2
Normal	Non-Lesion	trunk	39
Normal	Non-Lesion	arm	4
Normal	Non-Lesion	leg	4
Normal	Non-Lesion	neck	2

Supplementary Table 1. Details of skin samples.

Supplementary Table 2.

Disease	Number of times sampled on different time points	Number of patients
AD	1	113
AD	2	11
AD	3	5
AD	4	2
AD	5	2
AD	6	2
AD	7	5
AD	9	2
AD	10	2
AD	11	1
AD	12	2
AD	13	1
AD	14	2
AD	15	1
AD	16	3
AD	18	2
Normal	1	24
Normal	2	2
Psoriasis	1	18

Supplementary Table 2. Number of samples and patients sampled multiple times.

Supplementary Table 3.

Local symptom	Severity score	Number of samples
erythema	0	71
erythema	1	237
erythema	2	175
erythema	3	34
erythema	NA	12
papulation	0	483
papulation	1	31
papulation	2	3
papulation	NA	12
induration	0	342
induration	1	158
induration	2	9
induration	3	8
induration	NA	12
excoriation	0	466
excoriation	1	38
excoriation	2	13
excoriation	NA	12
lichenification	0	314
lichenification	1	153
lichenification	2	31
lichenification	3	31

NA; no available data

Supplementary Table 3. Local symptoms of sampled skin.

Supplementary Table 4.

Reference	treatment	Fisher's exact test		Common genes with highly-weighted genes of SKITm10
		p-value	Odds ratio (95%CI)	
Swindell, et al.	IL-17A	3.09e-29	39.64 (23.90 – 63.78)	*SERPINB4 , S100A7A , PI3 , IVL , S100A9 , SERPINB3 , RHCG , KLK6 , CNFN , LCE3D , HBEGF , IL36G , CYP4F22 , LIPG , SLC5A1 , IL36RN , ENDOU , S100A7 , PRDM1 , SPRR2B , TCN1 , ALOX12B , FAM43A , SPRR2D , PLA2G3*
Nograles, et al.	IL-17	1.62e-10	40.26 (15.81 – 90.62)	*SERPINB4 , S100A8 , PI3 , S100A9 , RHCG , S100A7 , CRABP2 , SPRR2D*
Jiang, et al.	IL-17A	6.10e-16	38.41 (18.91 – 72.92)	*S100A7A , S100A8 , PI3 , S100A9 , SPRR2A , RHCG , LCE3A , HEPHL1 , PLA2G4D , IL36G , S100A7 , SPRR2B , SPRR2D*
	IL-17C	5.11e-05	53.78 (9.27 – 218.85)	*S100A7A , SPRR2A , IL36G*
	TNFa	1.70e-20	13.11 (8.30 – 20.06)	*S100A8 , PI3 , S100A9 , SPRR2A , RHCG , CNFN , LCE3A , LCE3D , OASL , HBEGF , LCE3E , HEPHL1 , IL36G , MXD1 , TYMP , TRPV3 , UPP1 , SLC5A1 , PRDM1 , SLC28A3 , SERPINB2 , SPRR2B , PPIF , CDSN , SPRR2D , PLA2G3 , RNF222 , CRCT1*
Gupta, et al.	IL17-A	7.19e-35	20.60 (13.87 – 30.10)	*SERPINB4 , S100A7A , S100A8 , PI3 , GJB2 , SPRR1A , S100A9 , SERPINB3 , SPRR2A , RHCG , SPRR1B , GJB6 , CNFN , TGM1 , LCE3D , OASL , HBEGF , HEPHL1 , PLA2G4D , IL36G , SULT2B1 , TYMP , SLPI , TRPV3 , SLC5A1 , IL36RN , S100A7 , PRDM1 , PRSS22 , PLA2G4E , SLC28A3 , SPRR2B , CALML3 , CRABP2 , ALOX12B , SPRR2D , MX1 , MPZL2 , RNF222 , KLK9*
	TNFa	9.80e-21	7.84 (5.34 – 11.31)	*SERPINB4 , S100A8 , PI3 , S100A9 , SPRR2A , RHCG , DSC2 , LCE3D , HBEGF , IGFL1 , IL1RN , HEPHL1 , ODC1 , IL36G , SULT2B1 , TYMP , FOSL1 , PHLDA2 , SLPI , TRPV3 , UPP1 , SLC5A1 , IL36RN , ANXA1 , PRDM1 , DRAP1 , PRSS22 , CSTB , PLA2G4E , SLC28A3 , SERPINB2 , SPRR2B , GOLGA7B , KLK10 , PNP , TUBB6 , GLTP , PPIF , SPRR2D , CDKN1A , CRCT1*
Tollenaere, et al.	IL-17A	3.05e-26	22.31 (14.02 – 34.47)	*SERPINB4 , S100A7A , SERPINB3 , SPRR2A , RHCG , LCE3A , DDIT4 , OASL , HBEGF , LCE3E , HEPHL1 , PLA2G4D , IL36G , FOSL1 , TRPV3 , UPP1 , HK2 , IL36RN , PRDM1 , PRSS22 , SPRR2B , TCN1 , PRSS27 , PPIF , FAM43A , SPRR2D , KLK9 , FCHSD1*
	IL-17C	1.00e+00	0.00 (0.00 – 851.00)	-
	IL-17F	5.24e-22	27.65 (16.12 – 45.54)	*SERPINB4 , S100A7A , GJB2 , SERPINB3 , SPRR2A , RHCG , LCE3A , HEPHL1 , PLA2G4D , IL36G , TRPV3 , UPP1 , HK2 , IL36RN , PRSS22 , SPRR2B , TCN1 , PRSS27 , SPRR2D , KLK9 , FCHSD1*

Italicized text indicates gene names.

Supplementary Table 4. Enrichment analysis of highly weighted genes in SKITm10.
Fisher's exact test was performed with the reference data set and highly weighted genes of SKITm10.

Supplementary Table 5.

Reference	treatment	Fisher's exact test		Common genes with marker genes of SKITm10
		p-value	Odds ratio (95%CI)	
Swindell, et al.	IL-17A	3.59e-06	47.64 (11.44 - 149.83)	*SERPINB4, PI3, IVL, LIPG*
Nograles, et al.	IL-17	4.37e-04	75.24 (8.18 - 332.56)	*SERPINB4, PI3*
Jiang, et al.	IL-17A	1.31e-03	42.48 (4.69 - 183.02)	*LCE3A, PI3*
	IL-17C	1	0 (0 - 514.02)	-
	TNFa	2.68e-04	15.31 (3.71 - 47.72)	*UPP1, MXD1, LCE3A, PI3*
Gupta, et al.	IL17-A	4.19e-03	10.53 (1.97 - 36.58)	*SPRR1A, PI3, SERPINB4*
	TNFa	9.92e-06	12.53 (4.22 - 33.87)	*IGFL1, UPP1, IL1RN, PI3, DSC2, PHLDA2, SERPINB4*
Tollenaere, et al.	IL-17A	9.96e-04	17.63 (3.29 - 61.39)	*UPP1, LCE3A, SERPINB4*
	IL-17C	1	0 (0 - 7358.56)	-
	IL-17F	2.21e-04	29.92 (5.56 - 104.92)	*UPP1, LCE3A, SERPINB4*

Italicized text indicates gene names.

Supplementary Table 5. Enrichment analysis of marker genes in SKITm10.
Fisher's exact test was performed with the reference data set and marker genes of SKITm10.

Supplementary Table 6.

	AD	Psoriasis	Normal	Total
Number of samples	416 (Lesion: 246, Non-Lesion: 170)	36 (Lesion: 18, Non-Lesion: 18)	49	501
Number of patients	150	18	26	
Age (mean ±SD)	42.1 (31.0–43.2)	62.3 (52.5–78.0)	46.2 (34.6–57.9)	
Sex	Female: 45 Male: 105	Female: 4 Male: 14	Female: 7 Male: 19	
EASI (mean ±SD)	18.4 (6.1–30.7)	-	-	
Treatment (n = number of samples)	Dupilumab (n = 0) Topical steroid (n = 326) Topical tacrolimus (n = 10) Topical JAK inhibitor (n = 4) Oral Cyclosporine (n = 34) nemolizumab (n = 2)	Topical steroid/vitD3 (n = 13) Topical vitD analog (n = 1) Adalimumab (n = 10) Guselkumab (n = 2) Ustekinumab (n = 2) Ixekizumab (n = 2) Risankizumab (n = 2)	-	

Supplementary Table 6. Patient demographics of cross-sectional study.

Supplementary Table 7.

Lesion / Non-Lesion	Region	Number of samples
Lesion	face	2
Lesion	neck	7
Lesion	trunk	237
Non-Lesion	face	1
Non-Lesion	trunk	169

Supplementary Table 7. Sampled regions from patients with AD in cross-sectional study.

Supplementary Table 8.

Number of sampled times on different dates	Number of patients
1	126
2	15
3	5
4	3
6	1

Supplementary Table 8. Sampling over multiple times from patients with AD in cross-sectional study.

Supplementary Table 9.

Patient ID	Sex	Baseline mEASI	mEASI 6 months after dupilumab treatment	EASI improvement rate at 6 months (%)
Pt01	M	8.4	0	100
Pt02	F	15	0.7	95.33
Pt03	M	14.7	1.5	89.8
Pt04	M	15.2	NA	NA
Pt05	F	18.8	4.8	74.47
Pt06	M	16.1	2.6	83.85
Pt07	M	26.4	2.2	91.67
Pt08	M	30.8	2	93.51
Pt09	M	33	3.4	89.7
Pt10	M	24.3	4.2	82.72
Pt11	F	24.2	6.8	71.9
Pt12	M	26	4.4	83.08
Pt13	M	17	8	52.94
Pt14	M	22.6	5.6	75.22
Pt15	M	20.6	9.6	53.4
Pt16	M	35.2	5.2	85.23
Pt17	M	17.2	10.8	37.21
Pt18	M	21.6	NA	NA
Pt19	M	24.8	10	59.68
Pt20	M	29.7	11.8	60.27
Pt21	M	28.8	15.6	45.83
Pt22	M	35.6	6.7	81.18
Pt23	M	39.8	9.2	76.88
Pt24	M	38.8	7.4	80.93

NA; no available data

mEASI: modified Eczema Area and Severity Index

Supplementary Table 9. Patient demographics in longitudinal study of dupilumab-treated AD patients.

Supplementary Table 10.

Gene Symbol	Assay ID	Dye Label
CCL18	Hs00268113_m1	FAM-MGB
CCL13	Hs00234646_m1	FAM-MGB
IL23A	Hs00372324_m1	FAM-MGB
CCL20	Hs00355476_m1	FAM-MGB
IL17C	Hs00171163_m1	FAM-MGB
IL13	Hs00174379_m1	FAM-MGB
CCL26	Hs00171146_m1	FAM-MGB
IL17A	Hs00174383_m1	FAM-MGB
IL17F	Hs01028648_m1	FAM-MGB
HPRT1	Hs02800695_m1	VIC-MGB

Italicized text indicates gene names.

Supplementary Table 10. List of qPCR assays.

Reference for Supplementary data file 4

1. Lefèvre-Utile, A. et al. Transcriptome-based identification of novel endotypes in adult atopic dermatitis. Allergy 77, 1486–1498 (2022).
2. Martin, P., Goldstein, J. D., Mermoud, L., Diaz-Barreiro, A. & Palmer, G. IL-1 Family Antagonists in Mouse and Human Skin Inflammation. Front. Immunol. 12, 652846 (2021).
3. Peng, G. et al. Experimental and Clinical Evidence Suggests That Treatment with Betacellulin Can Alleviate Th2-Type Cytokine-Mediated Impairment of Skin Barrier Function. Int. J. Mol. Sci. 23, (2022).
4. Nauroy, P. & Nyström, A. Kallikreins: Essential epidermal messengers for regulation of the skin microenvironment during homeostasis, repair and disease. Matrix Biology Plus 6-7, 100019 (2020).
5. Nakahigashi, K. et al. Upregulation of aquaporin-3 is involved in keratinocyte proliferation and epidermal hyperplasia. J. Invest. Dermatol. 131, 865–873 (2011).
6. Lu, Z. et al. IL-20 promotes cutaneous inflammation and peripheral itch sensation in atopic dermatitis. FASEB J. 36, e22334 (2022).
7. Köten, B. et al. RNase 7 Contributes to the Cutaneous Defense against Enterococcus faecium. PLoS One 4, e6424 (2009).
8. Wang, S. et al. Single cell transcriptomics of human epidermis identifies basal stem cell transition states. Nat. Commun. 11, 1–14 (2020).
9. Swindell, W. R. et al. RNA-Seq Analysis of IL-1B and IL-36 Responses in Epidermal Keratinocytes Identifies a Shared MyD88-Dependent Gene Signature. Front. Immunol. 9, 80 (2018).
10. Belzberg, M. et al. Prurigo Nodularis Is Characterized by Systemic and Cutaneous T Helper 22 Immune Polarization. J. Invest. Dermatol. 141, 2208–2218.e14 (2021).
11. Wongvibulsin, S. et al. Transcriptomic analysis of atopic dermatitis in African Americans is characterized by Th2/Th17-centered cutaneous immune activation. Sci. Rep. 11, 11175 (2021).
12. Janes, S. M. et al. PI3-kinase-dependent activation of apoptotic machinery occurs on commitment of epidermal keratinocytes to terminal differentiation. Cell Res. 19, 328–339 (2009).
13. Tollenaere, M. A. X. et al. Signalling of multiple interleukin (IL)-17 family cytokines via IL-17 receptor A drives psoriasis-related inflammatory pathways. Br. J. Dermatol. 185, 585–594 (2021).
14. Cheng, J. B. et al. Transcriptional Programming of Normal and Inflamed Human Epidermis at Single-Cell Resolution. Cell Rep. 25, 871–883 (2018).
15. Tian, S. et al. Meta-analysis derived (MAD) transcriptome of psoriasis defines the 'core' pathogenesis of disease. PLoS One 7, e44274 (2012).
16. Sestito, R. et al. STAT3-dependent effects of IL-22 in human keratinocytes are counterregulated by sirtuin 1 through a direct inhibition of STAT3 acetylation. FASEB J. 25, 916–927 (2011).
17. Lambert, S., Swindell, W. R., Tsoi, L. C., Stoll, S. W. & Elder, J. T. Dual Role of Act1 in Keratinocyte Differentiation and Host Defense: TRAF3IP2 Silencing Alters Keratinocyte Differentiation and Inhibits IL-17 Responses. J. Invest. Dermatol. 137, 1501–1511 (2017).
18. Wolk, K. et al. IL-22 regulates the expression of genes responsible for antimicrobial defense, cellular differentiation, and mobility in keratinocytes: a potential role in psoriasis. Eur. J. Immunol. 36, 1309–1323 (2006).
19. Lobito, A. A. et al. Murine insulin growth factor-like (IGFL) and human IGFL1 proteins are induced in inflammatory skin conditions and bind to a novel tumor necrosis factor receptor family member, IGFLR1. J. Biol. Chem. 286, 18969–18981 (2011).
20. Ascensión, A. M., Fuertes-Álvarez, S., Ibañez-Solé, O., Izeta, A. & Araúzo-Bravo, M. J. Human Dermal Fibroblast Subpopulations Are Conserved across Single-Cell RNA Sequencing Studies. J. Invest. Dermatol. 141, 1735–1744.e35 (2021).
21. Solé-Boldo, L. et al. Single-cell transcriptomes of the human skin reveal age-related loss of fibroblast priming. Communications Biology 3, (2020).
22. Kagami, S. et al. Interleukin-4 and interleukin-13 enhance CCL26 production in a human keratinocyte cell line, HaCaT cells. Clin. Exp. Immunol. 141, 459–466 (2005).
23. Hoeck, J. & Woisetschläger, M. Activation of Eotaxin-3/CCL26 Gene Expression in Human Dermal Fibroblasts Is Mediated by STAT6. The Journal of Immunology 167, 3216–3222 (2001).
24. Chandriani, S. et al. Endogenously Expressed IL-13Rα2 Attenuates IL-13–Mediated Responses but Does Not Activate Signaling in Human Lung Fibroblasts. The Journal of Immunology 193, 111–119 (2014).
25. Kamsteeg, M. et al. Type 2 helper T-cell cytokines induce morphologic and molecular characteristics of atopic dermatitis in human skin equivalent. Am. J. Pathol. 178, 2091–2099 (2011).
26. Masuoka, M. et al. Periostin promotes chronic allergic inflammation in response to Th2 cytokines. J. Clin. Invest. 122, 2590–2600 (2012).
27. He, H. et al. Single-cell transcriptome analysis of human skin identifies novel fibroblast subpopulation and enrichment of immune subsets in atopic dermatitis. J. Allergy Clin. Immunol. 145, 1615–1628 (2020).
28. Veniaminova, N. A. et al. Niche-Specific Factors Dynamically Regulate Sebaceous Gland Stem Cells in the Skin. Dev. Cell 51, 326–340.e4 (2019).
29. Itabe, H., Yamaguchi, T., Nimura, S. & Sasabe, N. Perilipins: a diversity of intracellular lipid droplet proteins. Lipids Health Dis. 16, 83 (2017).
30. Rondini, E. A., Ramseyer, V. D., Burl, R. B., Pique-Regi, R. & Granneman, J. G. Single cell functional genomics reveals plasticity of subcutaneous white adipose tissue (WAT) during early postnatal development. Mol Metab 53, 101307 (2021).
31. Schittek, B. et al. Dermcidin: a novel human antibiotic peptide secreted by sweat glands. Nat. Immunol. 2, 1133–1137 (2001).
32. Viacava, P., Naccarato, A. G. & Bevilacqua, G. Spectrum of GCDFP-15 expression in human fetal and adult normal tissues. Virchows Arch. 432, 255–260 (1998).
33. Saarialho-Kere, U. K., Crouch, E. C. & Parks, W. C. Matrix metalloproteinase matrilysin is constitutively expressed in adult human exocrine epithelium. J. Invest. Dermatol. 105, 190–196 (1995).
34. Green, R. E. et al. A Draft Sequence of the Neandertal Genome. Science 328, 710–722 (2010).
35. Debeer, S. et al. Comparative histology and immunohistochemistry of porcine versus human skin. Eur. J. Dermatol. 23, 456–466 (2013).
36. Hamanaka, K. et al. De Novo Truncating Variants in the Last Exon of SEMA6B Cause Progressive Myoclonic Epilepsy. Am. J. Hum. Genet. 106, 549–558 (2020).